Developments in Synchrotron Instrumentation

A. Fitch

Synchrotron Radiation and Powder Diffraction

High intensity, collimation and λ tunability

$\Downarrow$

- High angular resolution, i.e. narrow peak widths;
- Rapid data collection / good statistics;
- Highly monochromatic X-rays, or energy dispersive;
- Narrow well defined intrinsic instrumental peak shape;
- Tunable: measure at absorption edges, or well away; optimise for the experiment.

Main technical developments since APD III

- Many new 3rd generation synchrotrons with powder diffractometers
- Analyser stages, multi-analyser stages, and multi-multi-analyser stages
- Mythen curved 1d PSD
- Dedicated insertion device sources (e.g. undulators)
- Hard energy operation
- Large 2d on-line detectors
- Focussing by refractive lenses
- Robotic sample changers
- Self aligning capillary spinners
- Radiation damage
- Beam heating

- + Raman, etc.
- Energy dispersive
- Etc.

Diamond, 3 GeV

Australian, 3 GeV

Petra, 6 GeV

Shanghai, 3 GeV

Accurate data ⇒ use Analyser crystal(s)

Cox, Hastings, Thomlinson,
Prewitt, Finger *et al.*
at BNL and CHESS.

X16C at NSLS

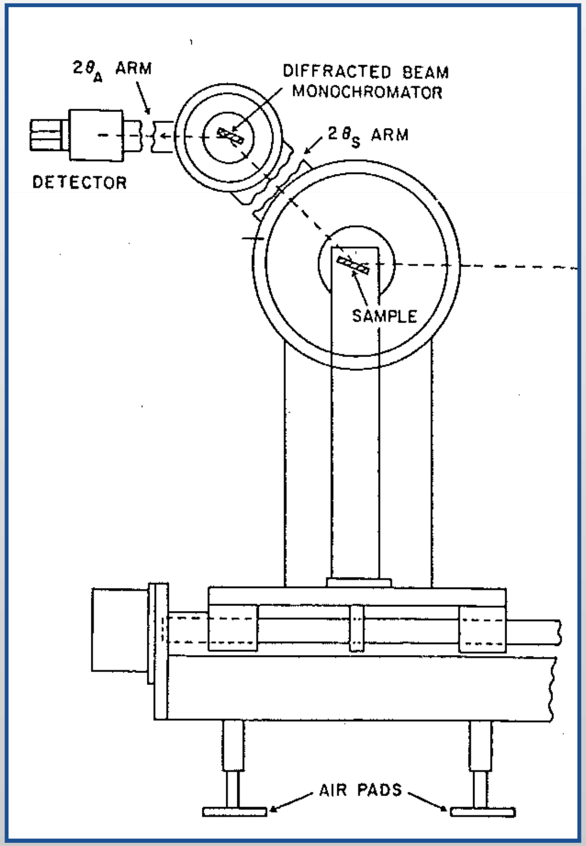

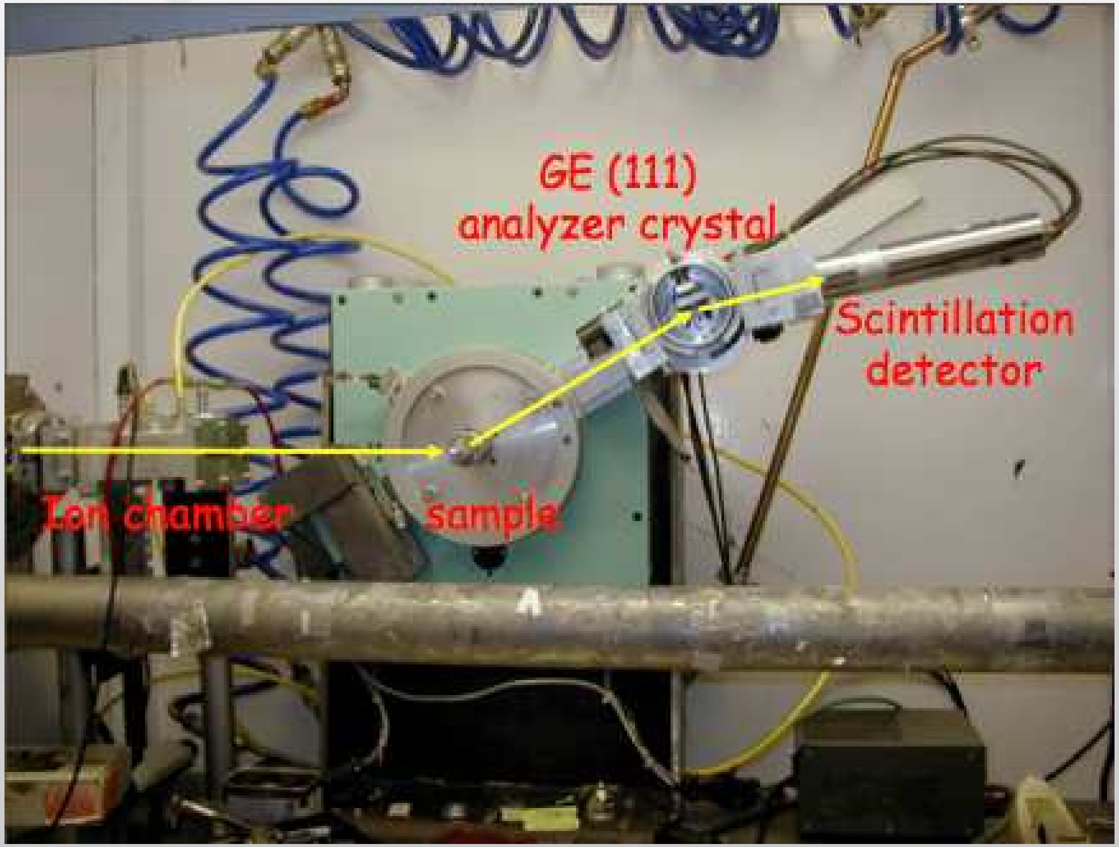

XPD diffractometer at LNLS, Brazil

No misalignment aberration

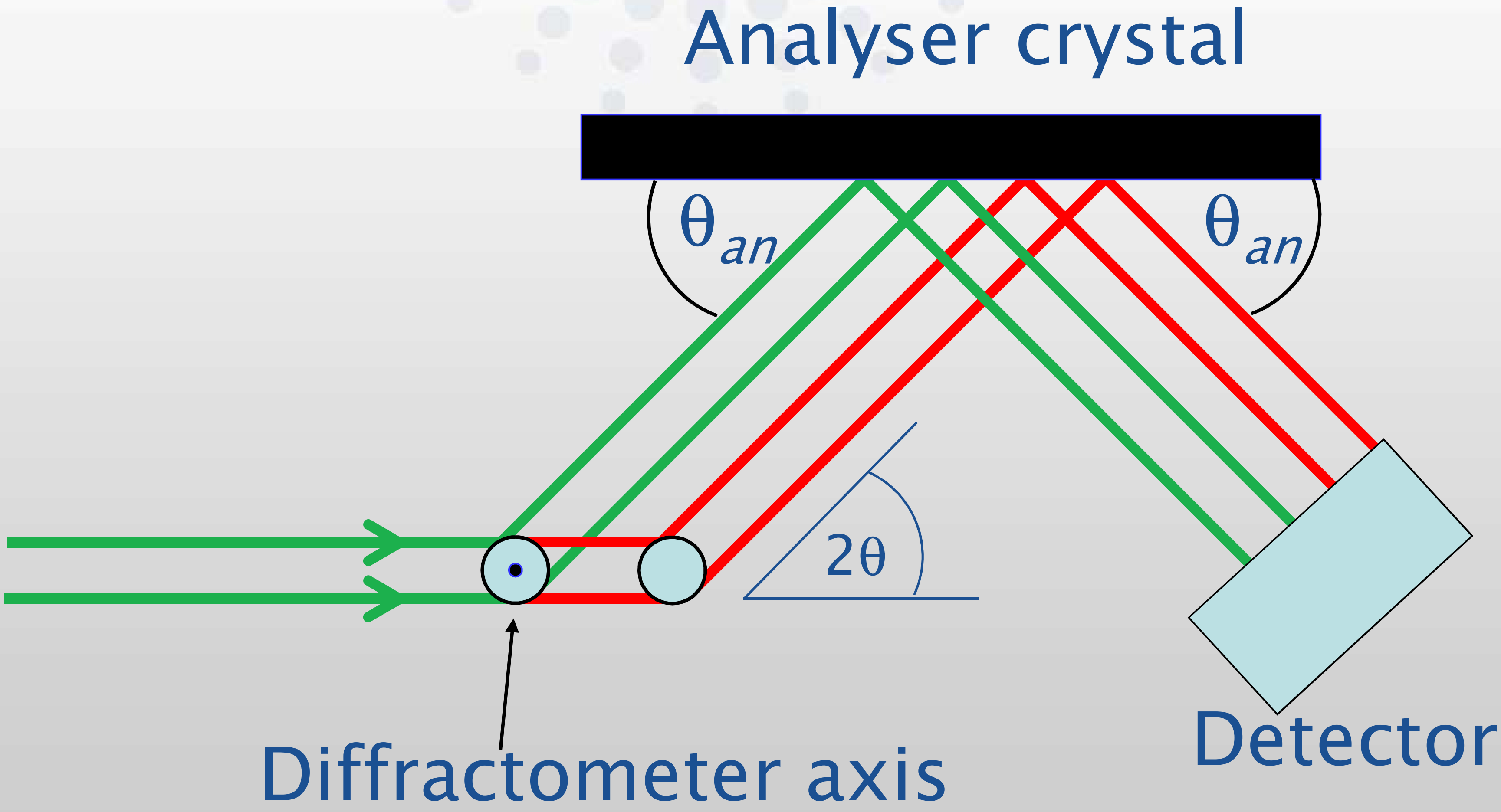

Analyser crystal

⇓

narrow peaks (sample limited) and accurate peak positions

Stringently defines a true 2θ *angle* rather than infers 2θ from the *position* of a slit or pixel of a PSD.

- Peak positions insensitive to misalignment, transparency, specimen-size/shape/surface effects, etc.;
- widths independent of any $\theta/2\theta$ parafocusing condition;
- supresses fluorescence, Compton, parasitic scatter.
- but SLOW   (scanning + very selective)

Nine channel multianalyser (MAC) stage

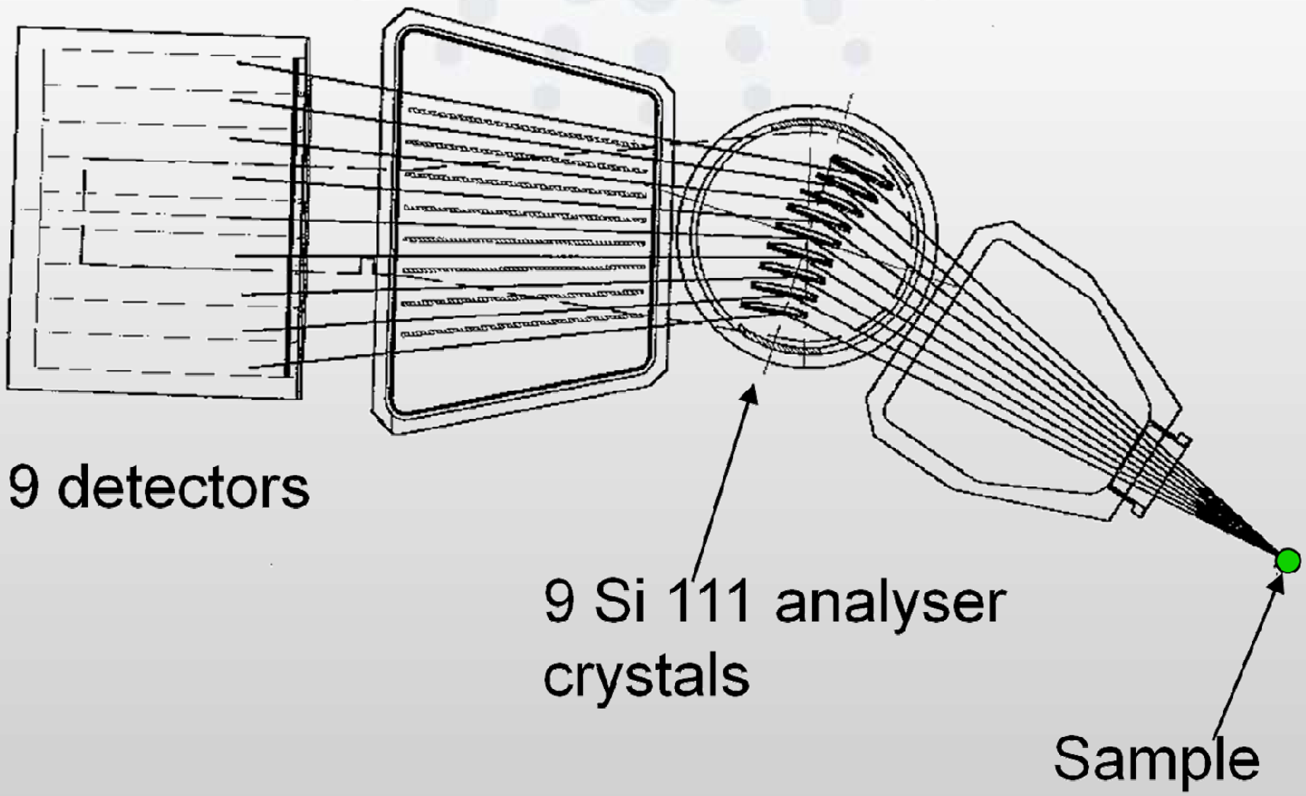

Thanks to J.-L. Hodeau, M. Anne, P. Bordet, A. Prat, CNRS, Grenoble

ID31 powder diffractometer, ESRF

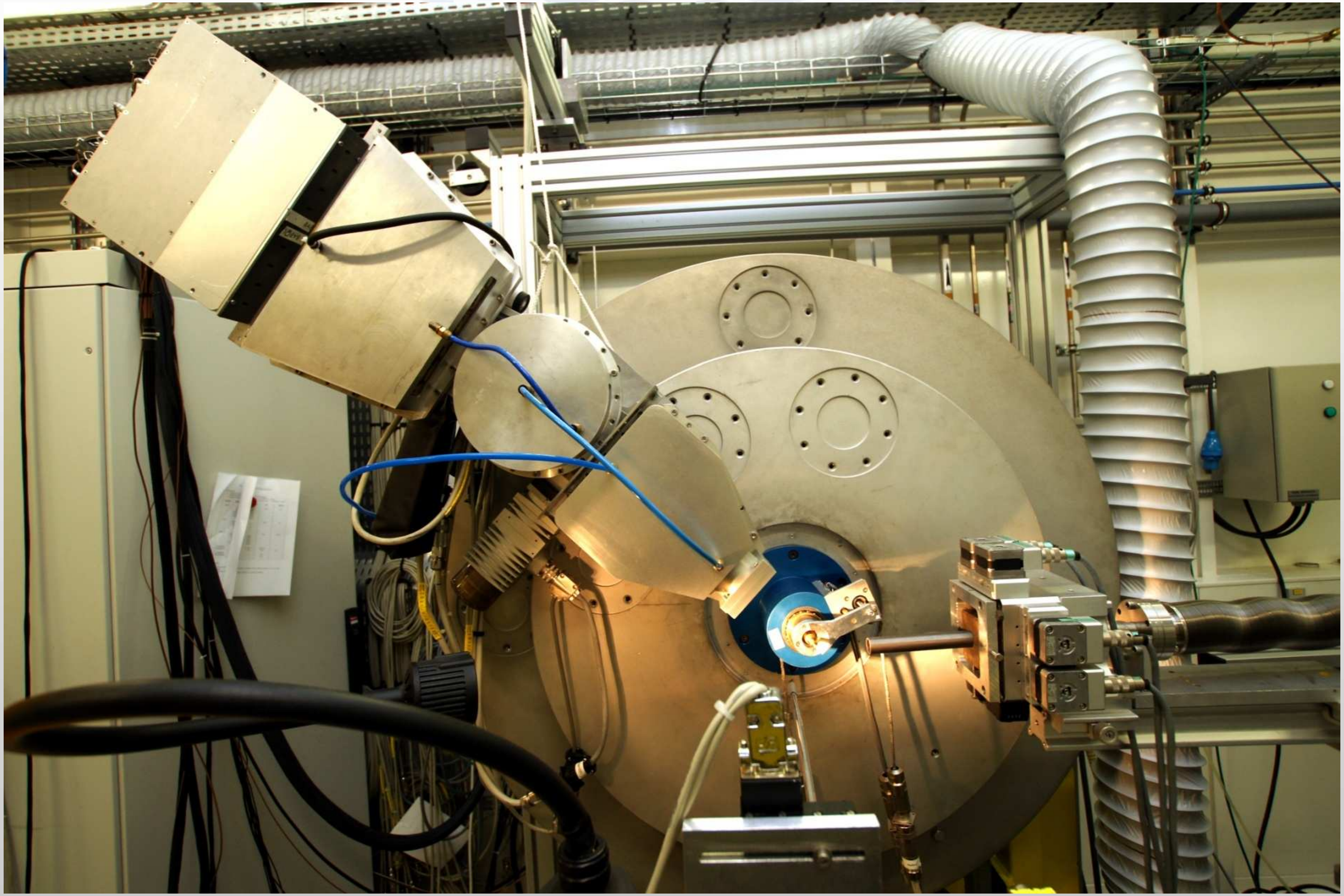

$\Delta\theta \approx 2^{\circ}$ $(\pm 0.1^{\circ})$

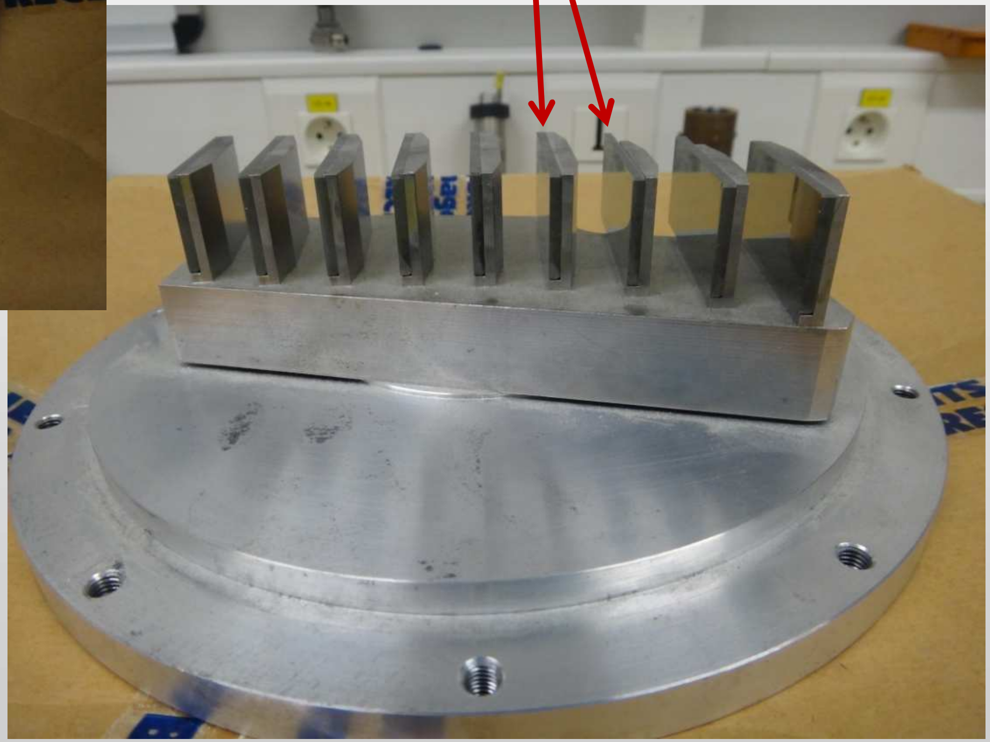

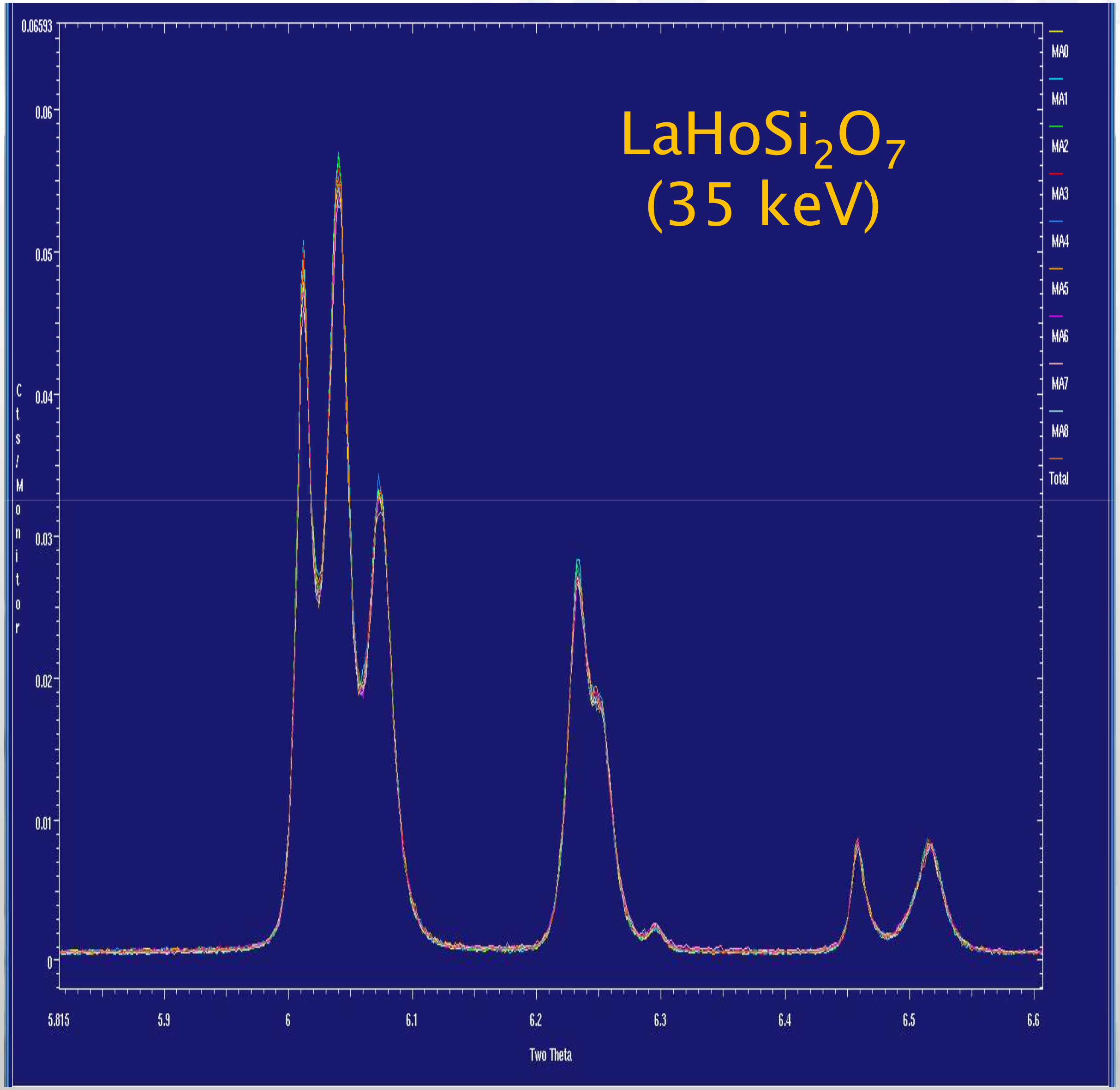

$\Delta\theta$	efficiency
8.05456833	1.01541956
5.96777827	1.08103083
3.98748335	1.11437177
2.04993441	1.04004295
0.00000000	0.92708866
−1.91689474	0.77755602
−4.03848485	1.02894135
−5.97433687	1.01258377
−7.99777260	1.00296507

$\Downarrow$

Variation affects hard-energy performance

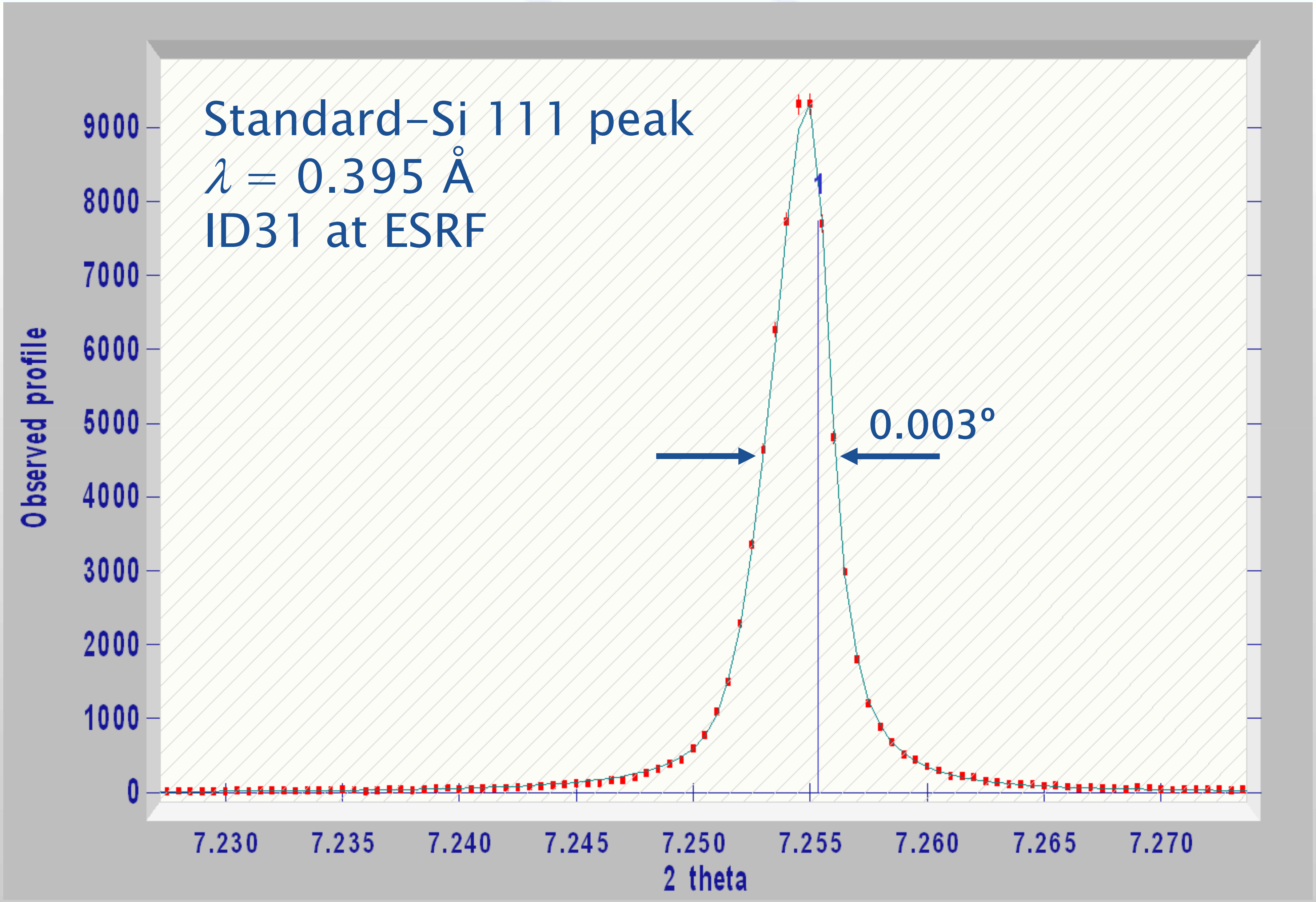
Standard-Si 111 peak
λ = 0.395 Å
ID31 at ESRF
0.003°
9000
8000
7000
6000
5000
4000
3000
2000
1000
0
Observed profile
7.230
7.235
7.240
7.245
7.250
7.255
7.260
7.265
7.270
2 theta

Beamline 11-BM at APS, 12 analyser crystals with individually adjustable θ and χ

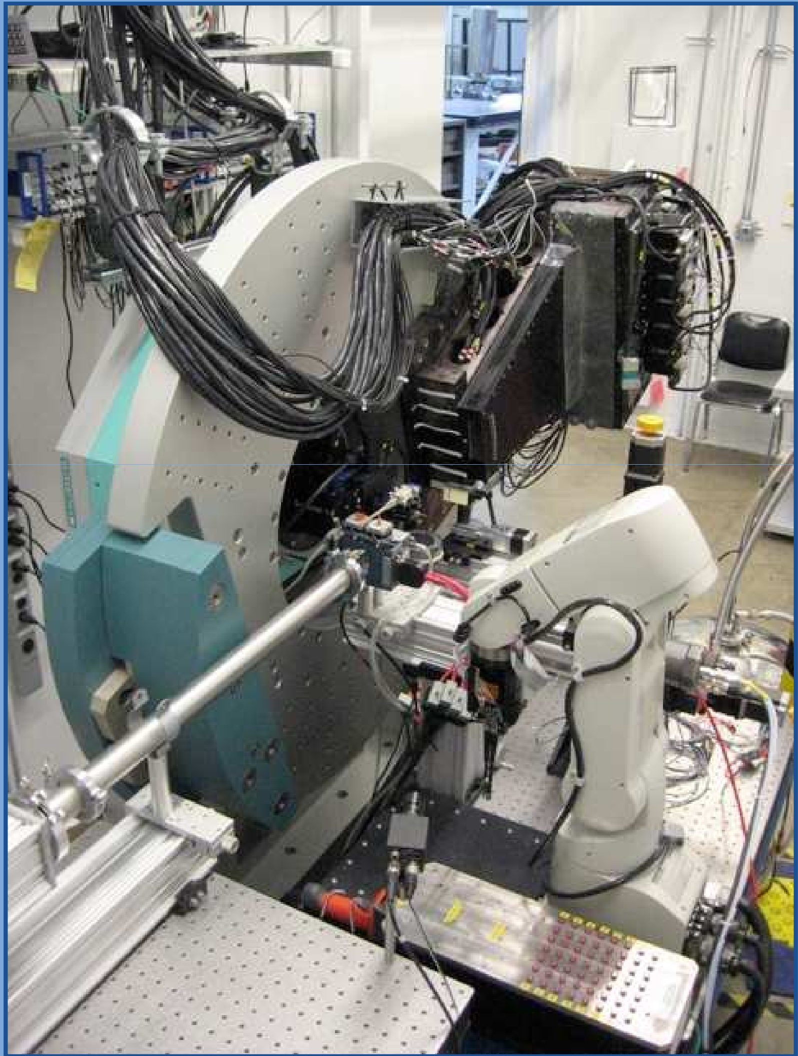

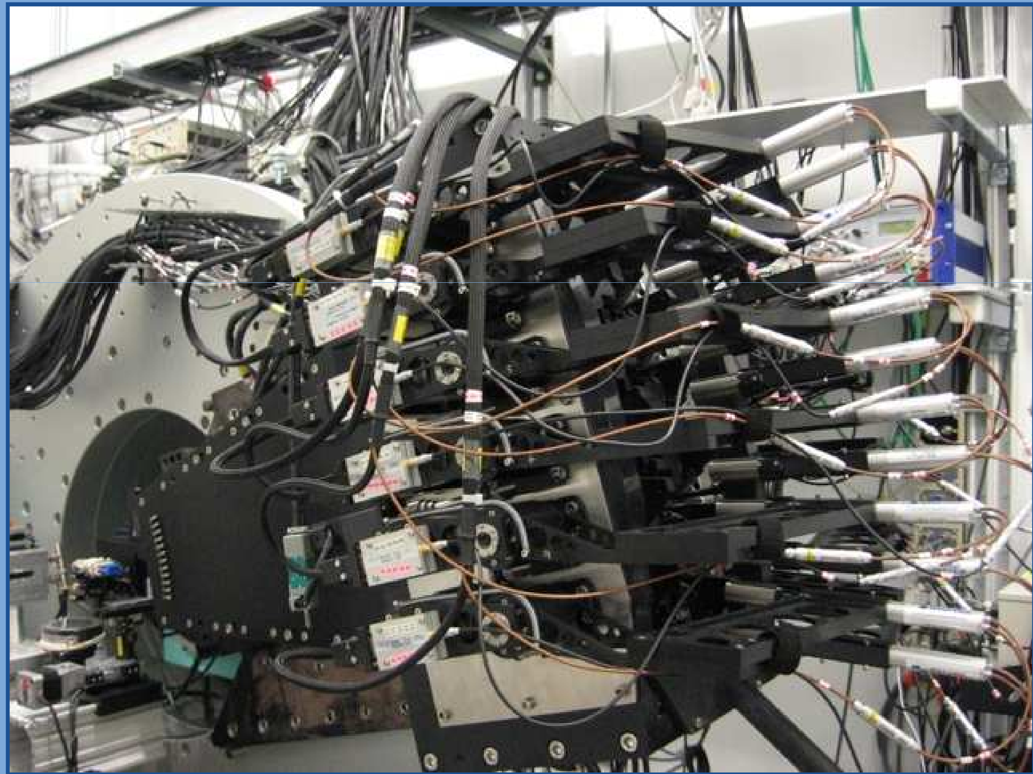

Beamline I11at Diamond, 45 analyser crystals

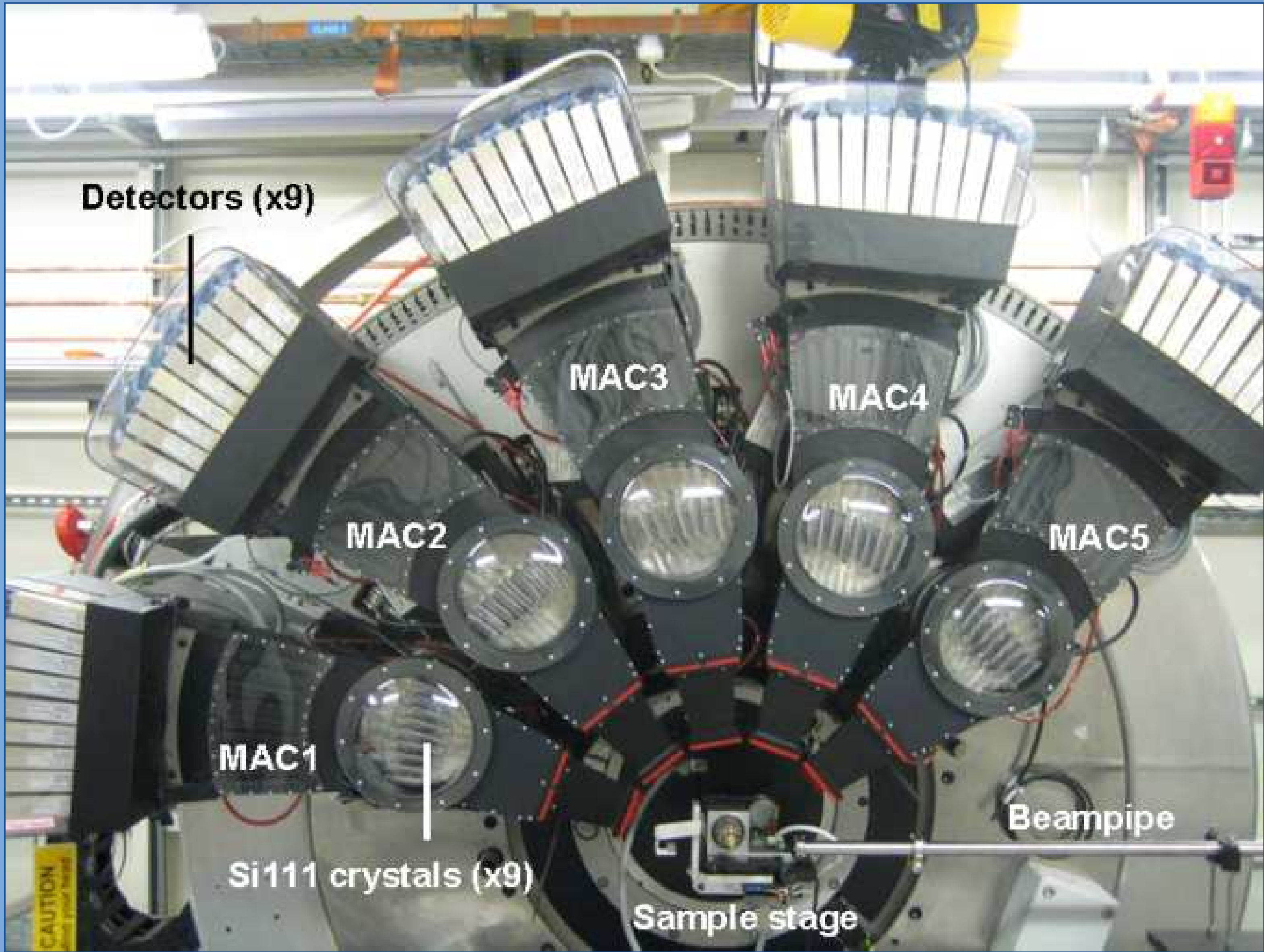

Mythen curved 1d PSD

- Developed at the Swiss Light Source.
- Modular Si-strip photon-counting detector
- 1280 channels, 50μm step, unit ≈4.83°, (≈0.004° $strip^{-1}$)
- Read out ≈250 μs
- The best 1d PSD for soft and intermediate energies
- Excellent statistical quality in minutes or even seconds
- 10 – 10^2 × faster than MAC

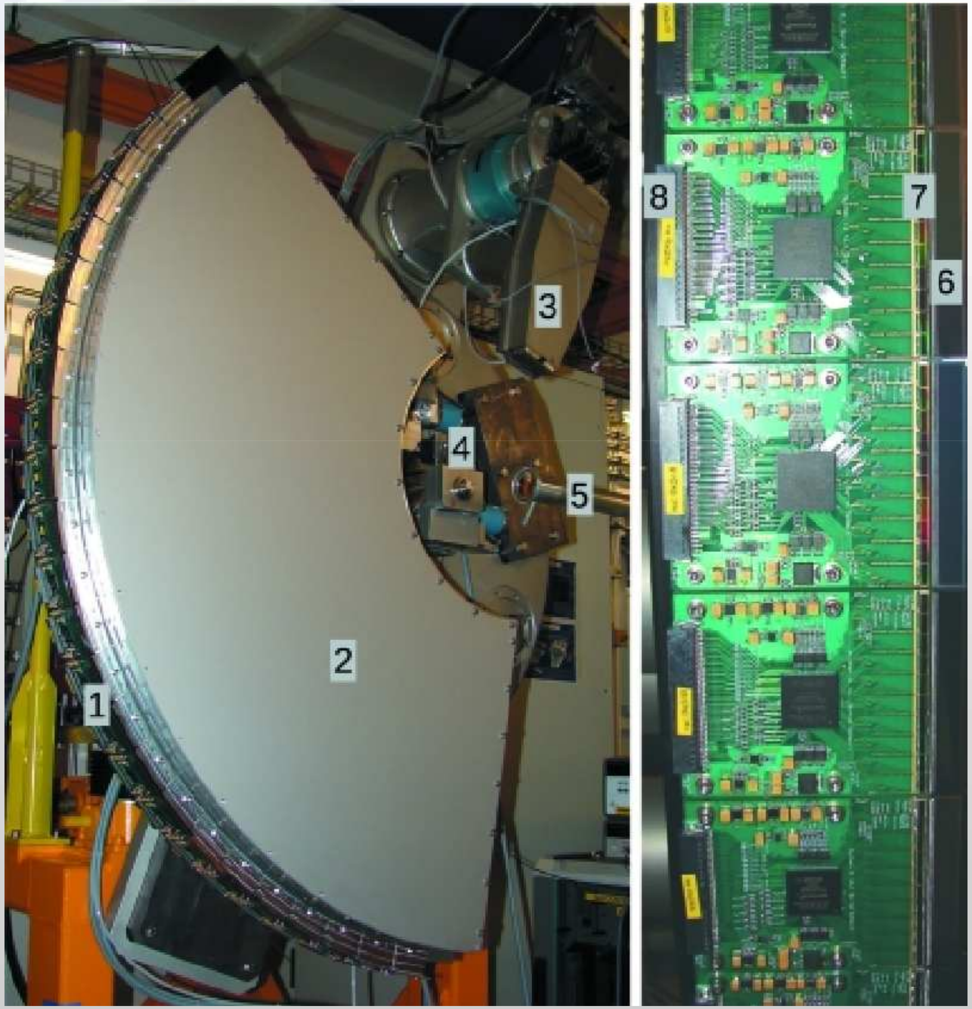

J. Synchr. Rad. 2010, 17, 653

Australian

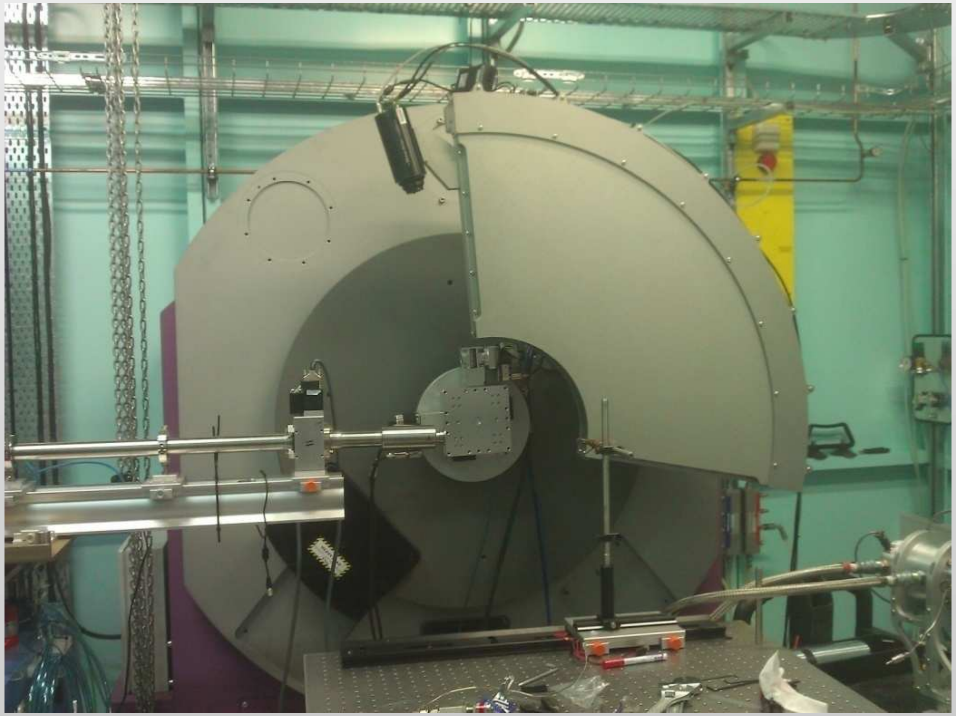

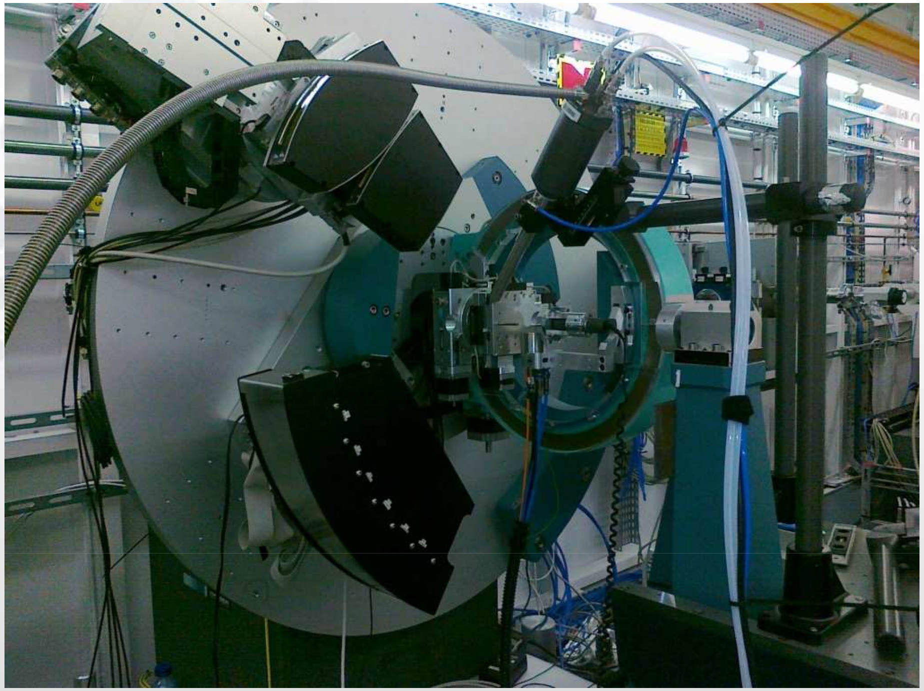

Alba (Spain)
Mythen and MAC
detectors

I11 Diamond

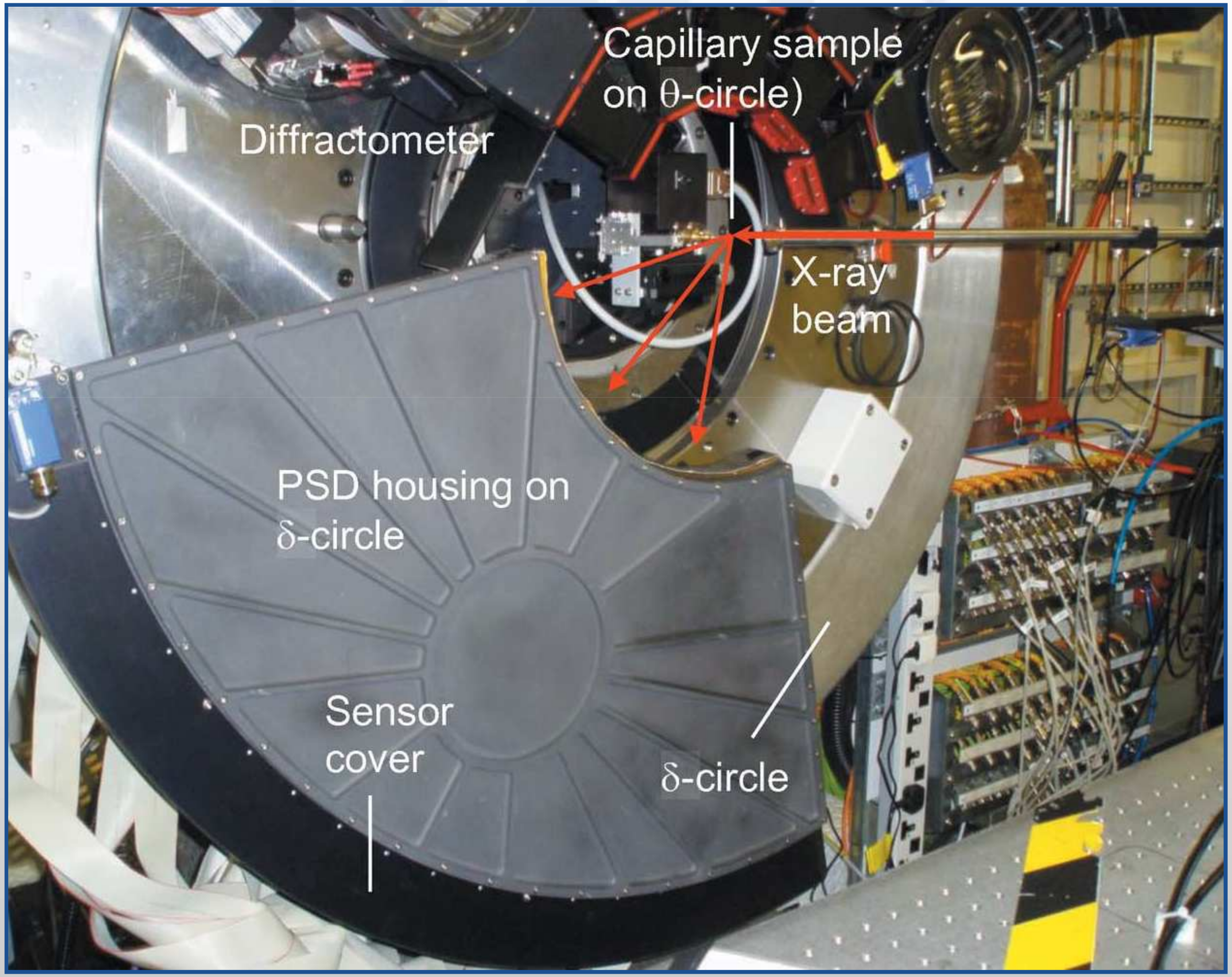

Thompson *et al.*, J. Sync. Rad. (2011)

Debye–Scherrer geometry
so susceptible
to aberrations

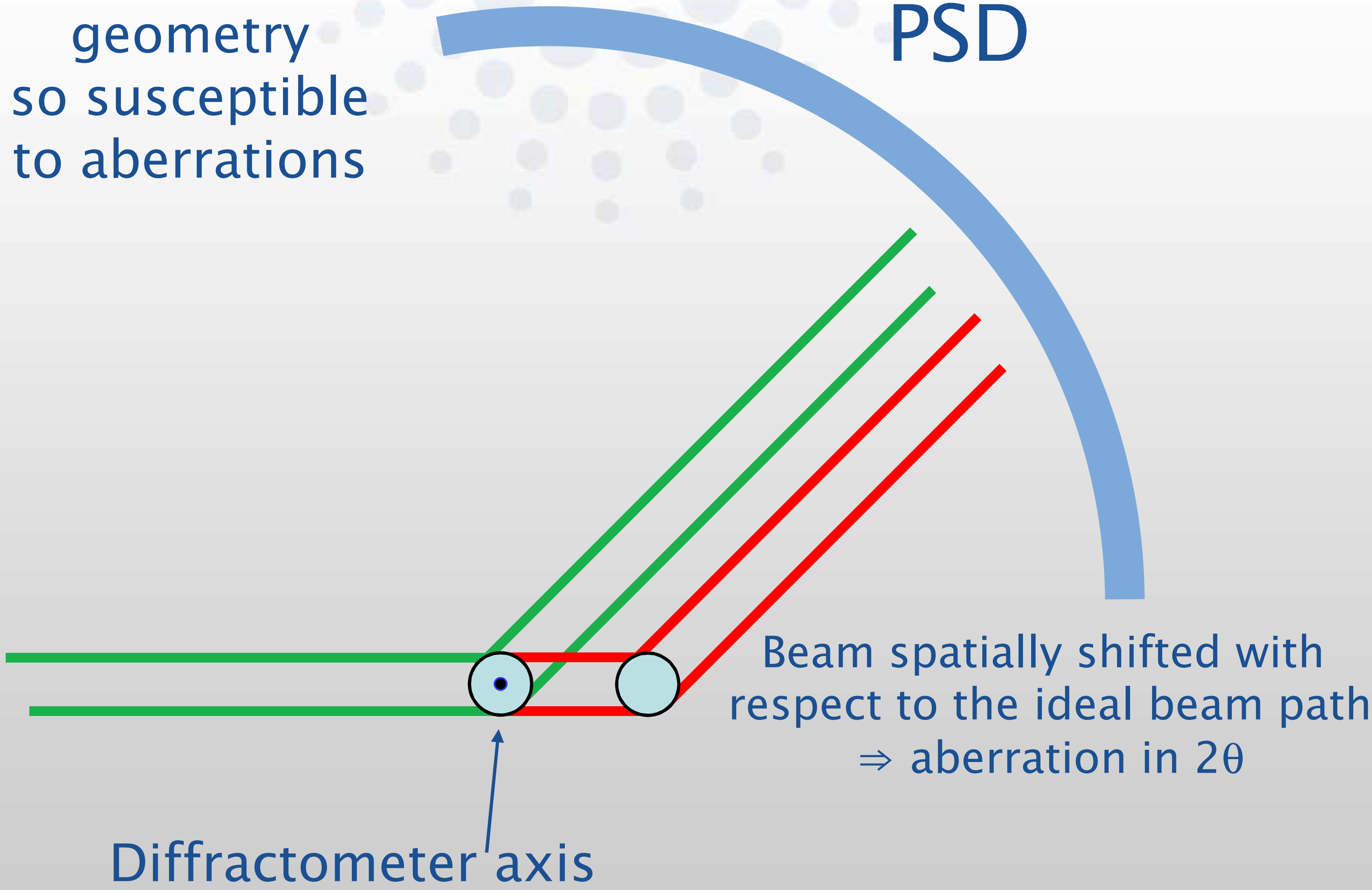

Ex-vacuum & in-vacuum undulators

ESRF (6 GeV) u35 undulator,11 mm gap

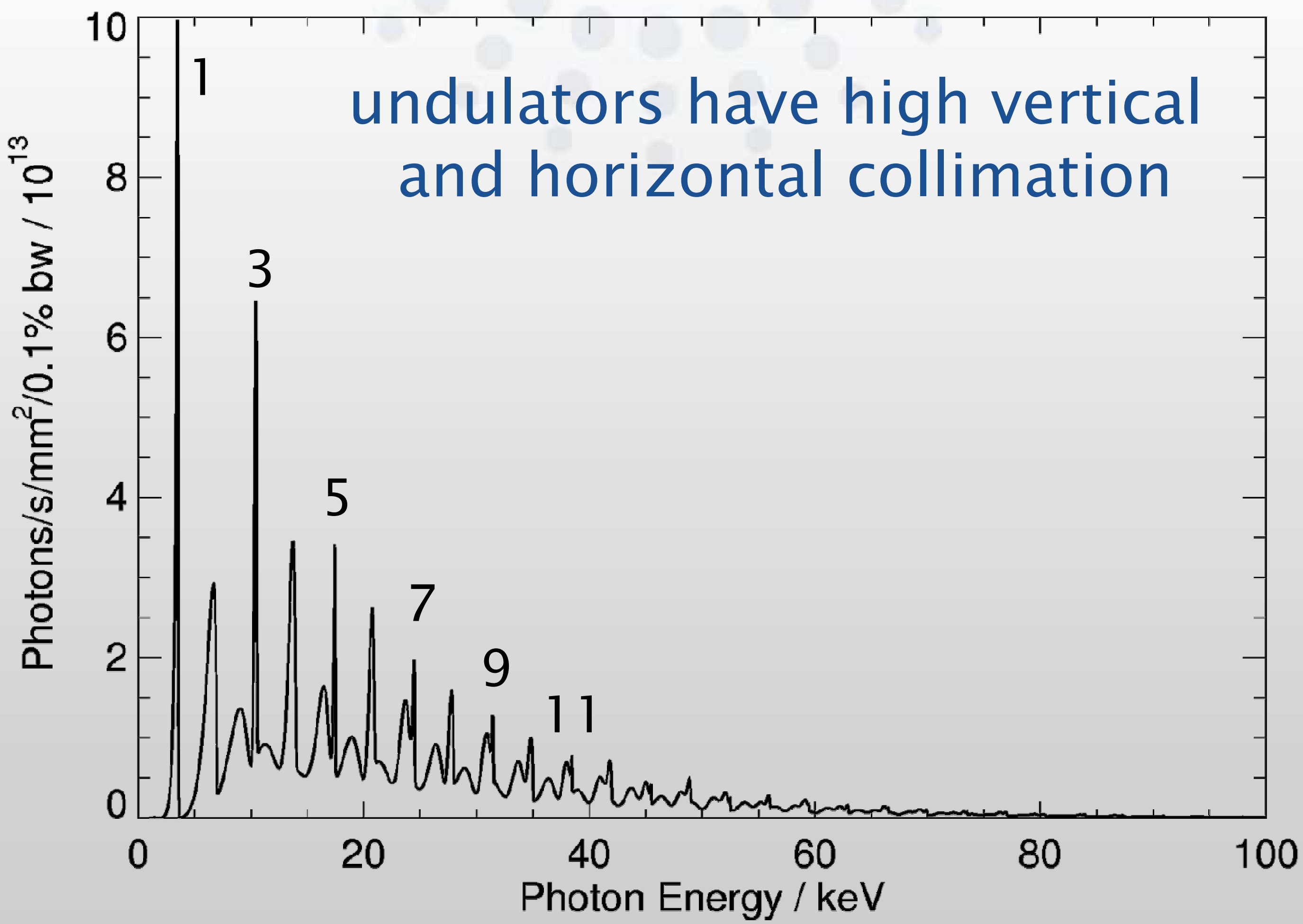

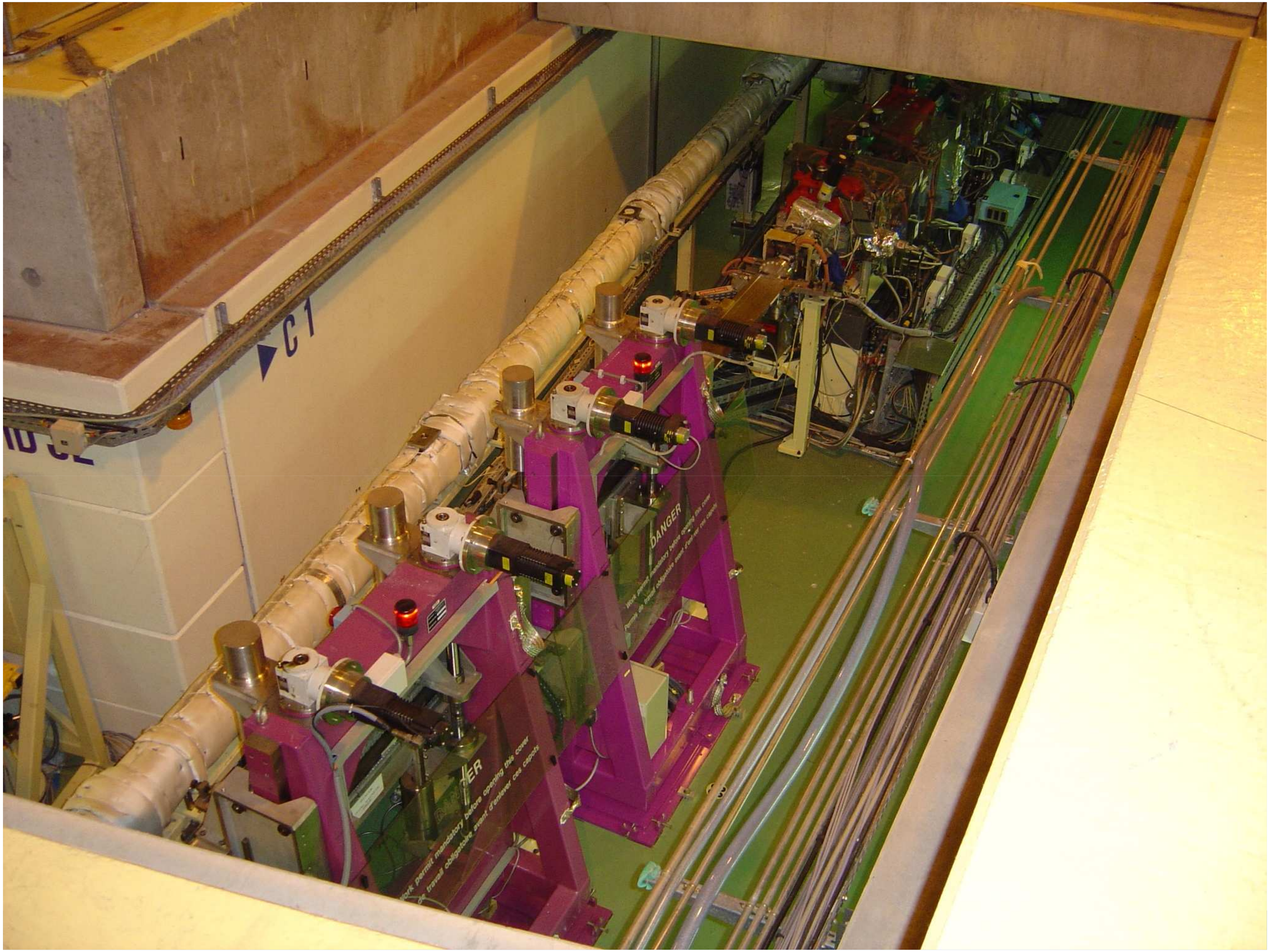

C1
DANGER
DANGER

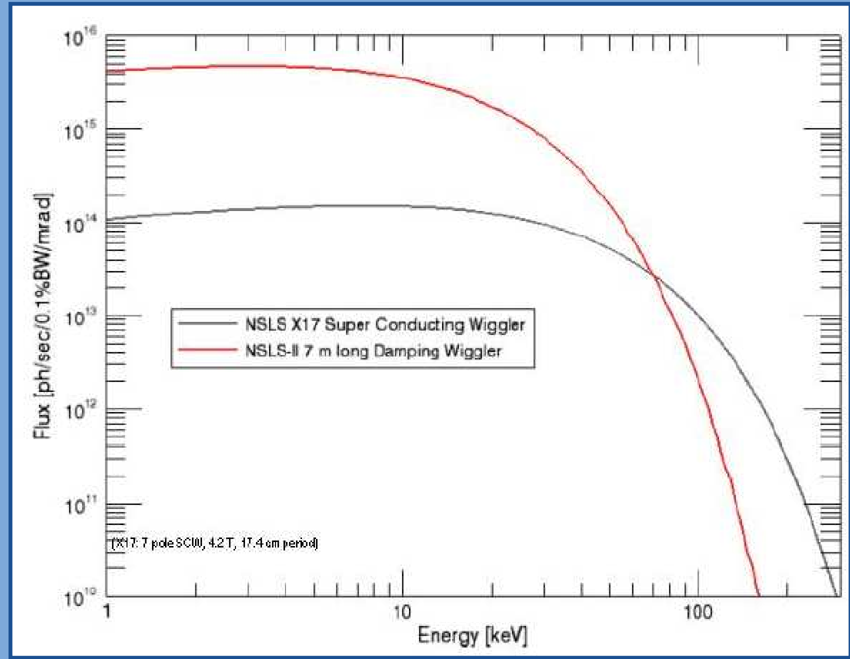

Damping wiggler for NSLS-II PD beamline (2014)

Hard energy operation

- “Hard energy” ≥ 30 keV ; $\lambda < 0.41$ Å
- Manageable absorption for all capillary samples
- Adjust capillary diameter ($2r$) so that $\mu r < 1.5$

Capilliary: scattered intensity *vs* μr

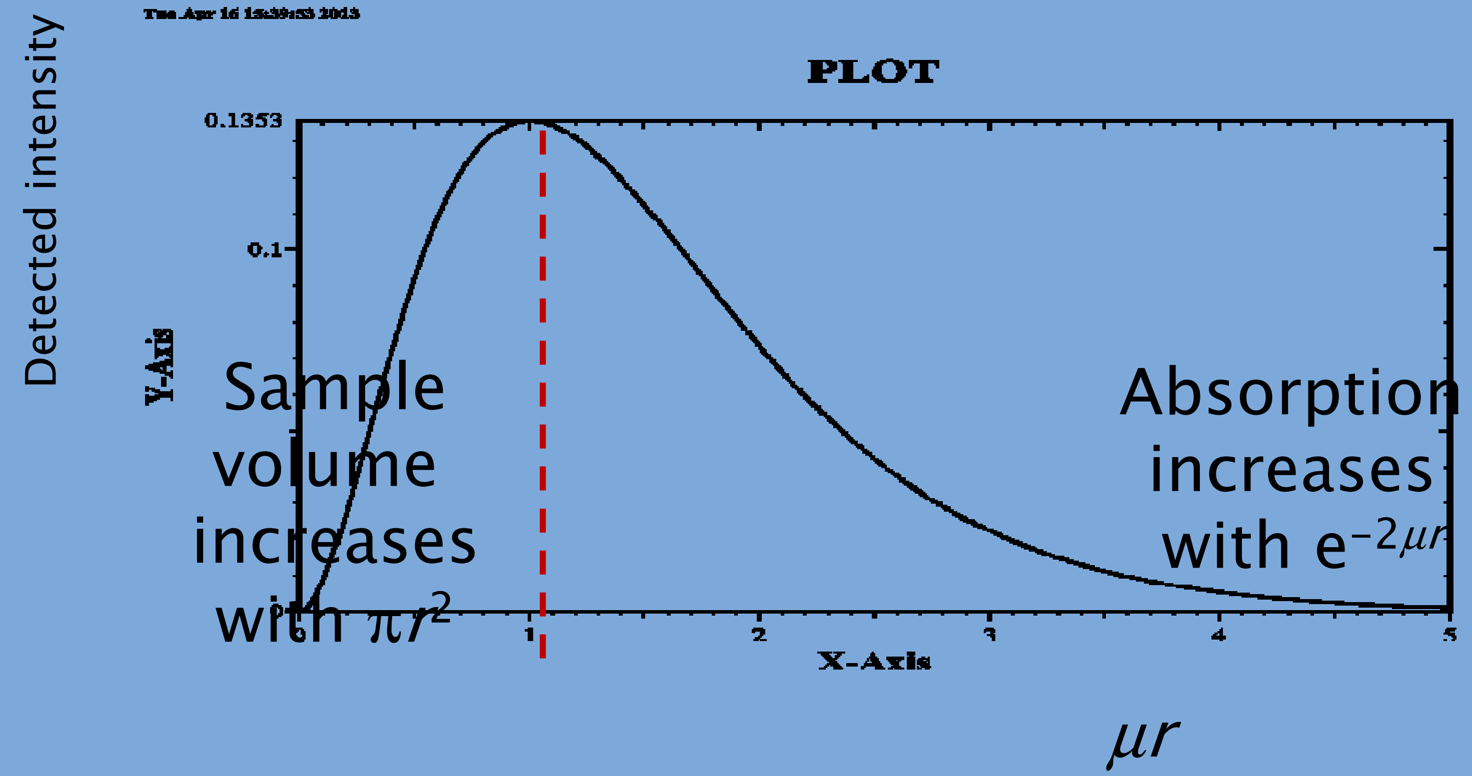

Hard energy operation

- Spinning capillary ⇒ fewer problems with preferred orientation so accurate intensities
- Capillary perfect for multi-analyser stage
- Reduced radiation damage ?
- PDF measurements
- Access useful K edges
- Less far to scan for a *Q* range
- Obtain full *Q* range in one shot with large 2d detector and ≥ 60 keV (e.g. fast-PDF)
- Downside: peaks are at lower angle ⇒ more asymmetry (unless using 2d detector)

2D detectors

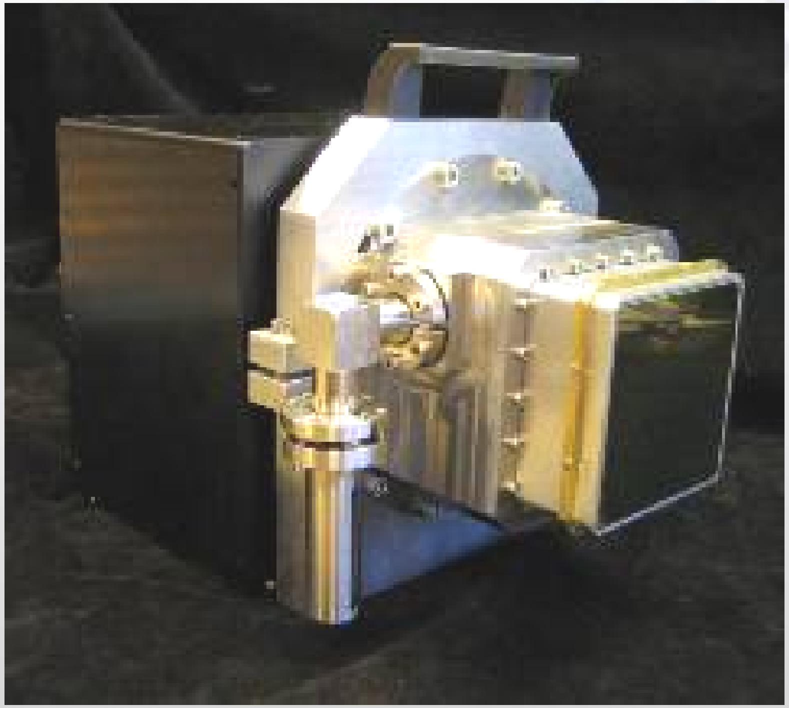

ESRF designed and constructed Frelon (Fast Readout Low Noise) camera
ID11 ESRF

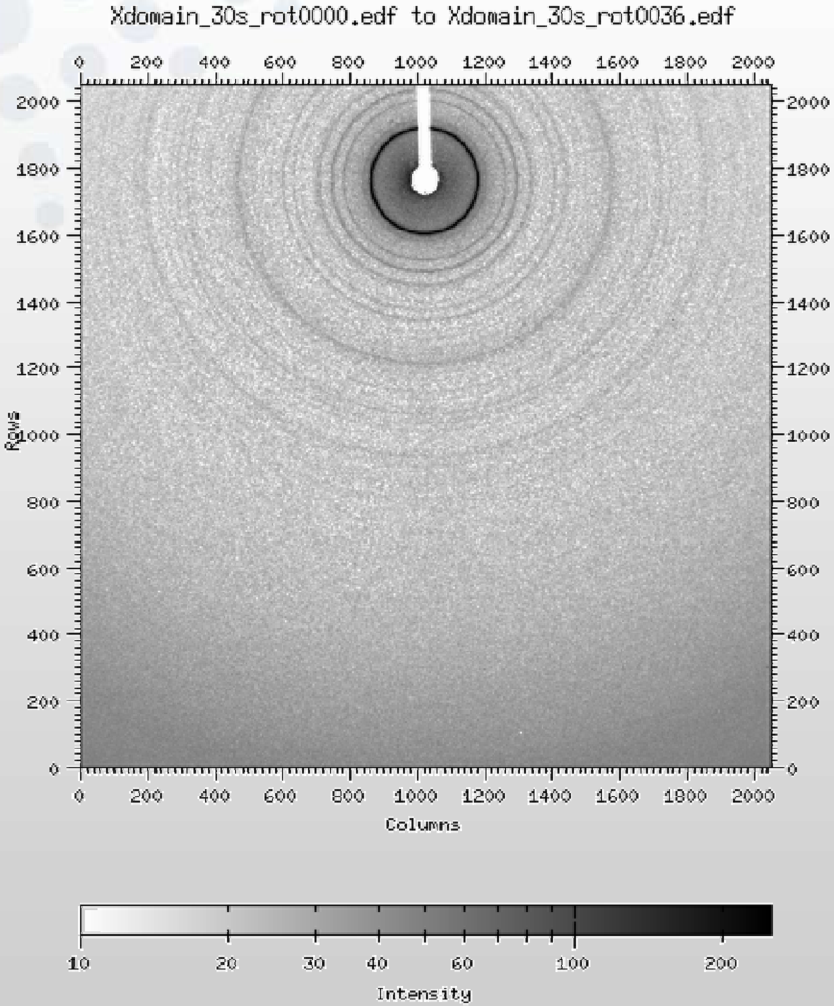

E = 42 keV

Medical imaging pixel detectors

$41 \times 41\ cm^2$
200 µm pixel
Readout 15 – 30 Hz

GE Healthcare detector (11-ID-B/C)

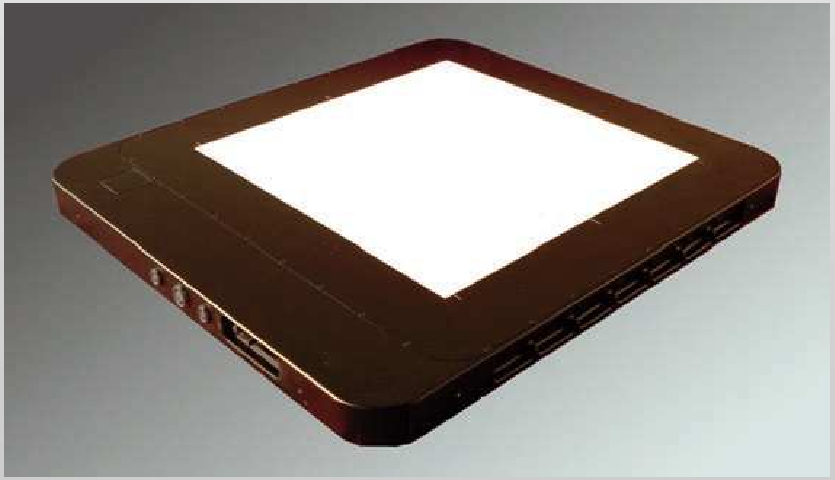

Perkin-Elmer (PETRA-III 11-ID-B/C)

Based on amorphous Si + CsI(Tl) scintillator

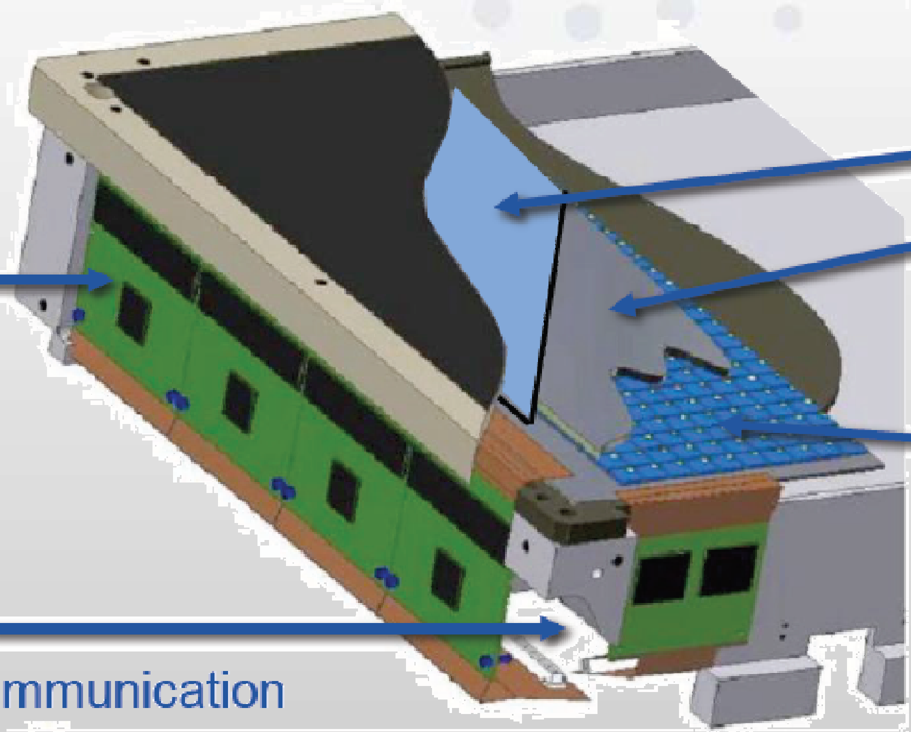

Rapid (30 Hz) PDF analysis nano-$PtO_2 \rightarrow Pt$

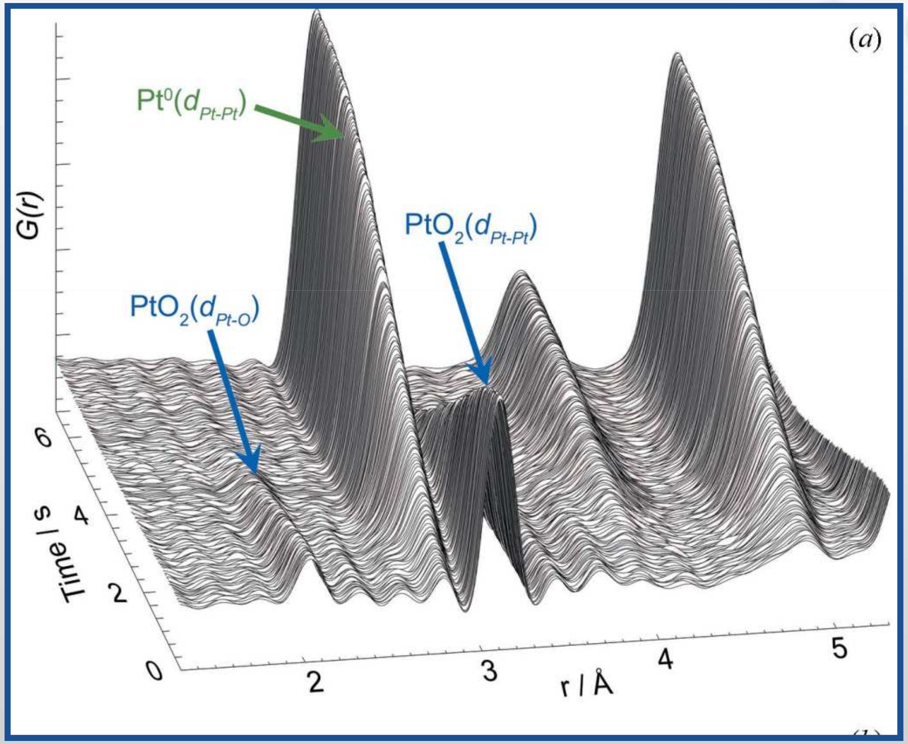

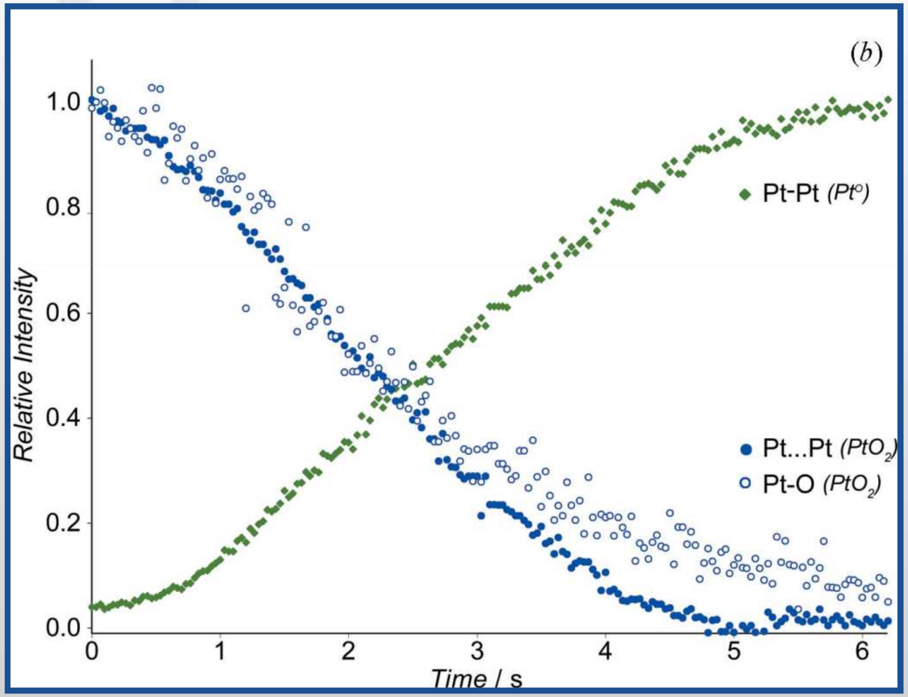

Chupas et al. J. Appl. Cryst. (2007) 40, 463

Flat panel detector

P02.1 Petra

multi-analyser

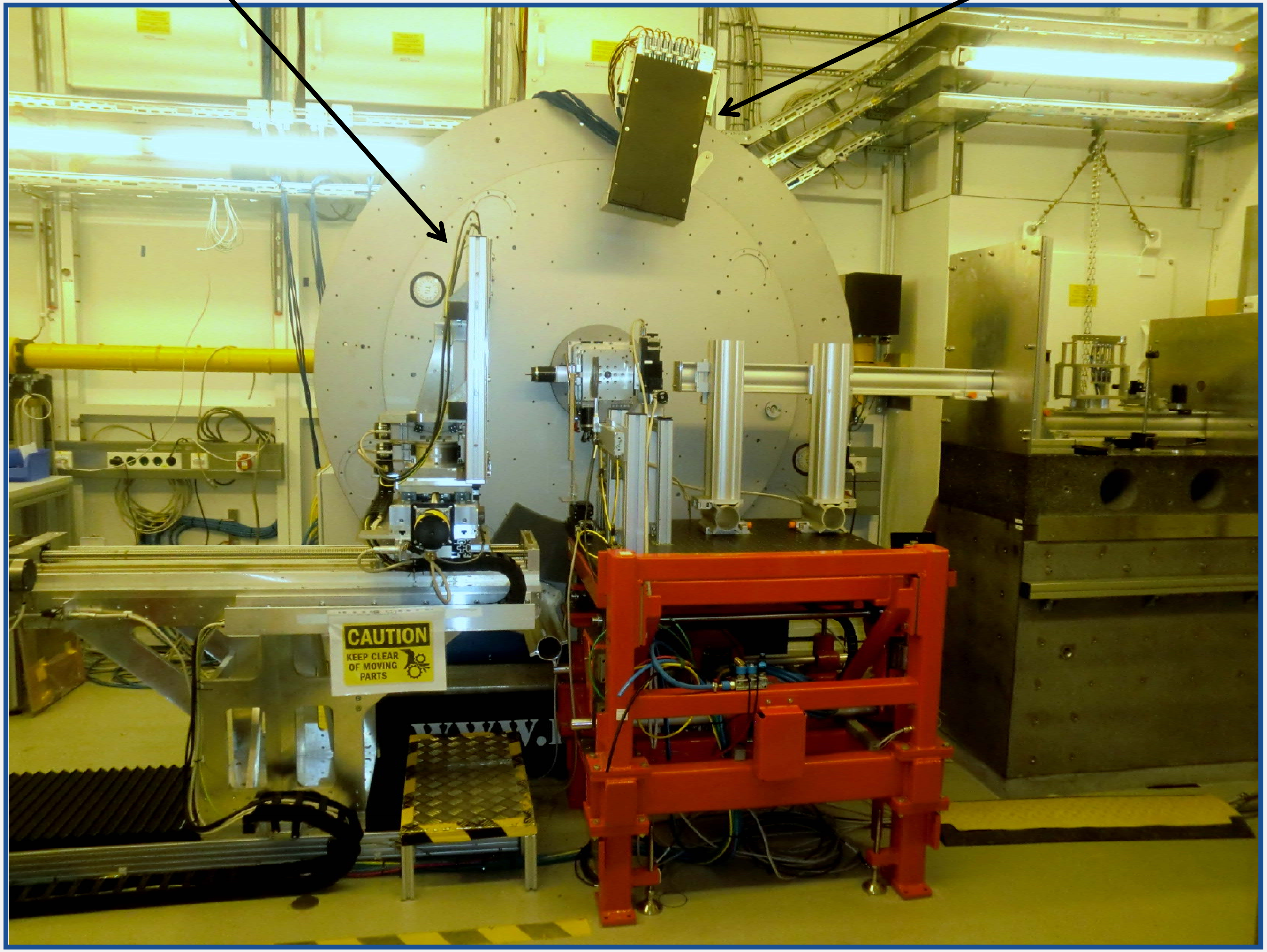

NSLS-II future powder station

3-circle diffractometer

2d flat panel detector

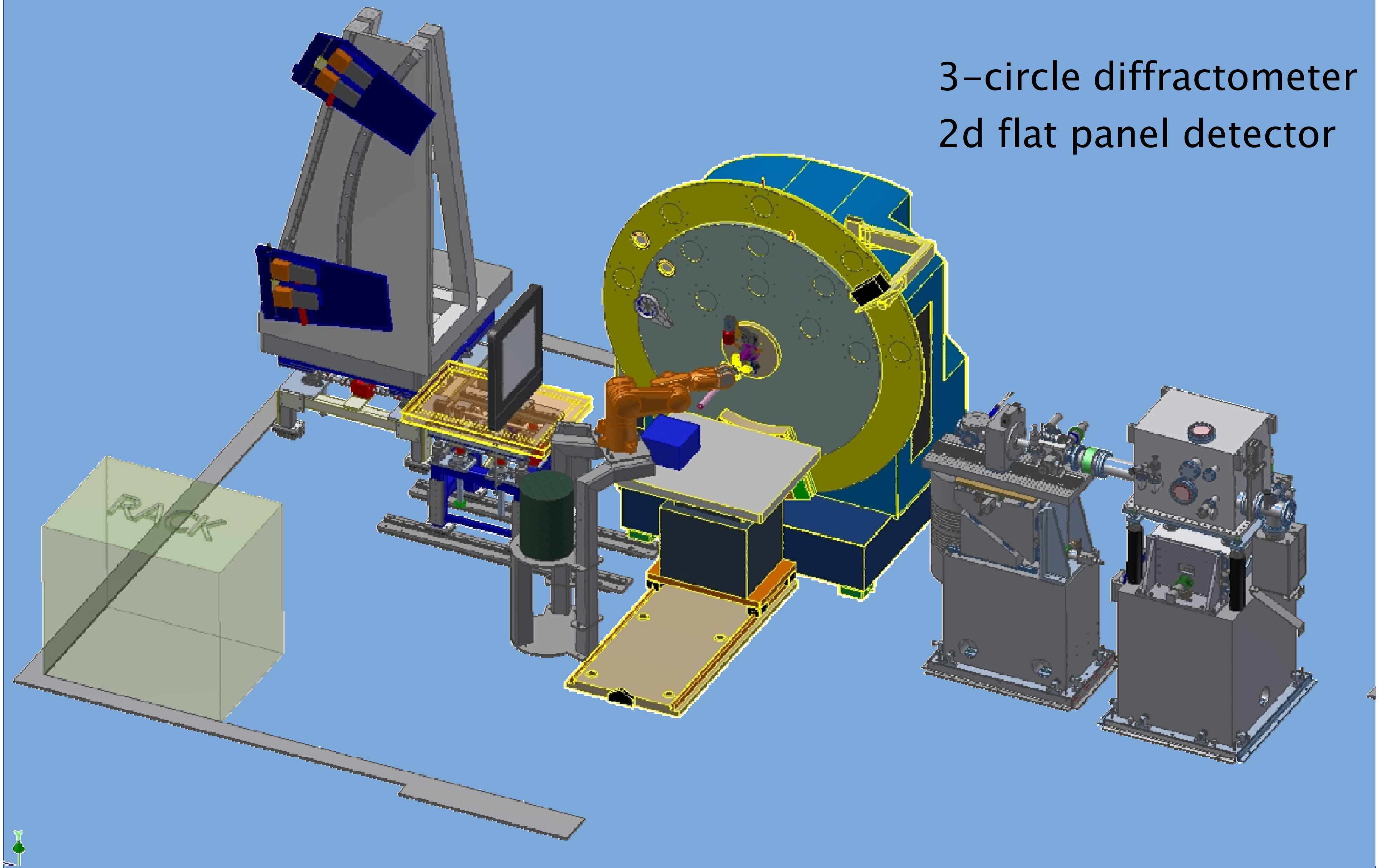

Si-based pixel detectors (structural biology)

Dectris 2M detector
BM01A
(SNBL)
ESRF

Bending magnet beamline

Study of PbS nanoparticles grown in annealed silicate glass

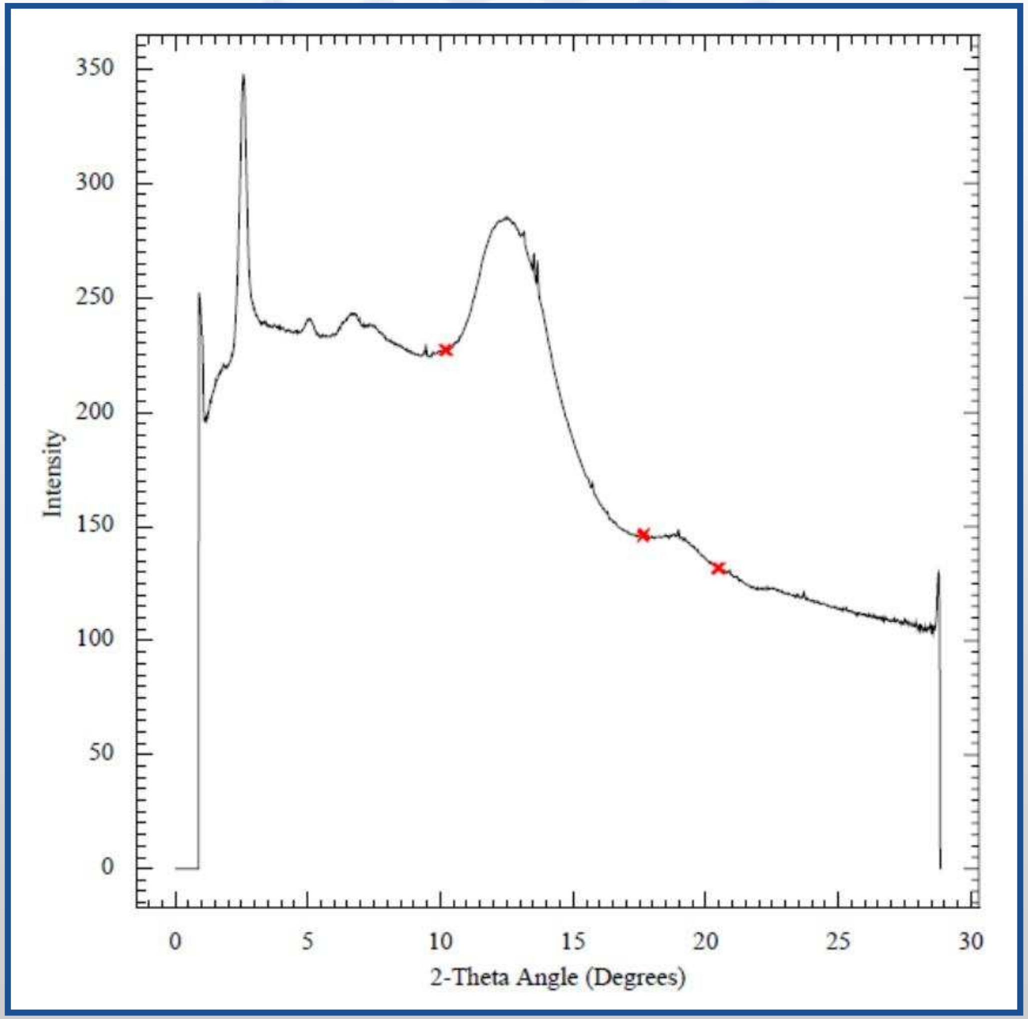

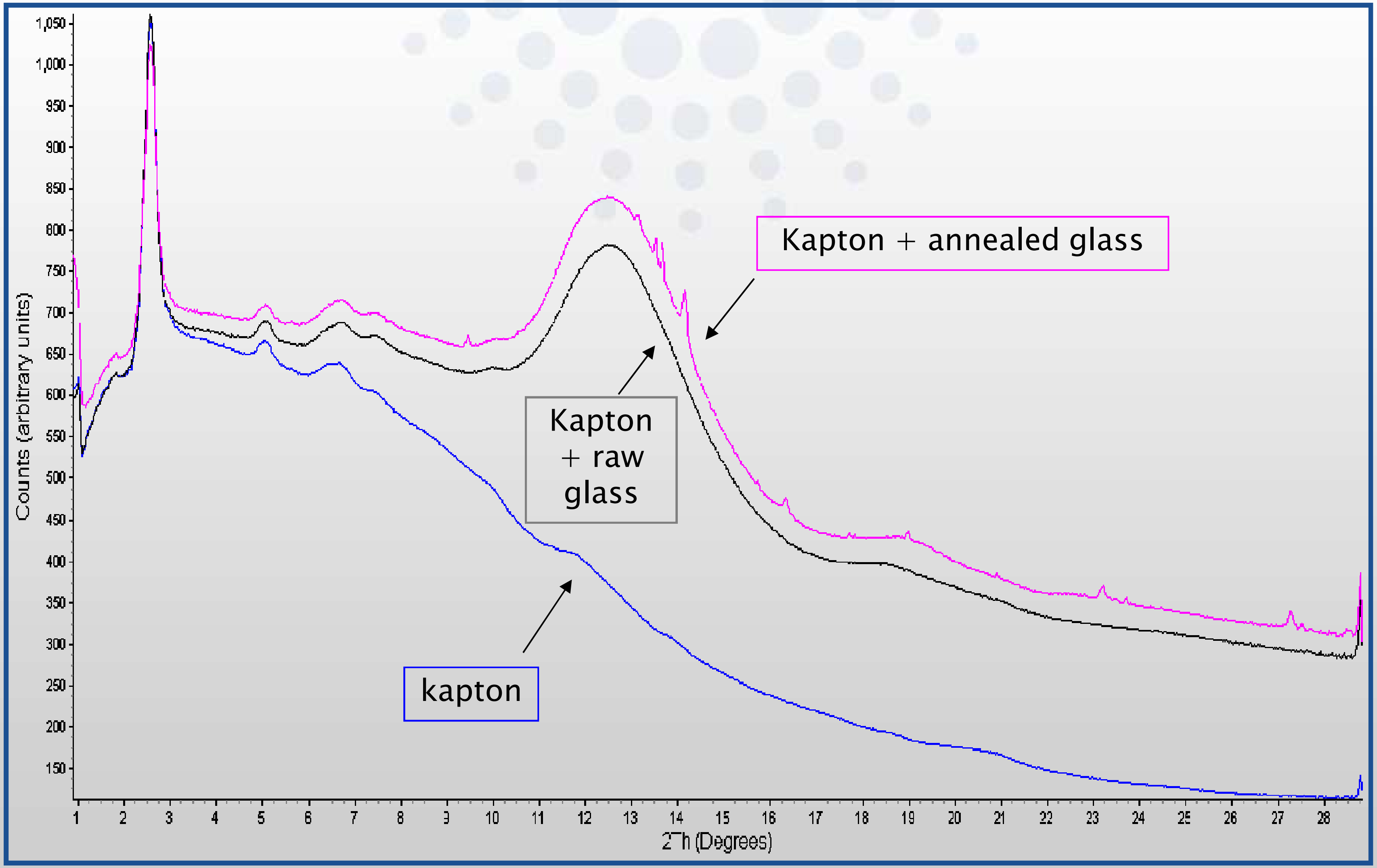
Counts (arbitrary units)
2Th (Degrees)
Kapton + annealed glass
Kapton + raw glass
kapton

	a (Å) expected	a (Å) fitted	Crystal size (nm) (Lorentzian shape)
Pb	4.9506	4.951( )	39.8
PbS	5.9315	5.9315 (fixed)	3.2

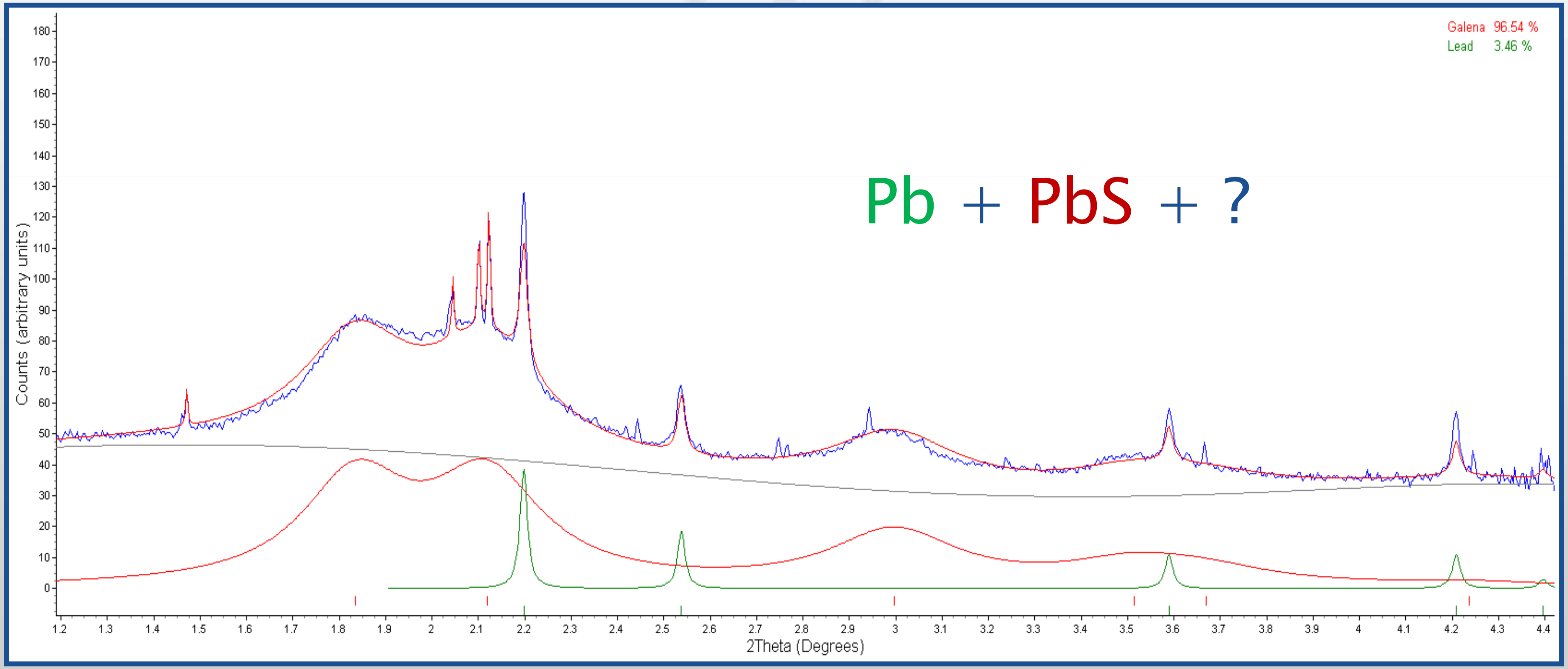

H.B. Stanley *et al.*

SAXS

Two log-normal sphere distributions

N=.002 R1=21.2 nm s=.077

N=12.4 R2=1.0 nm s=0.34

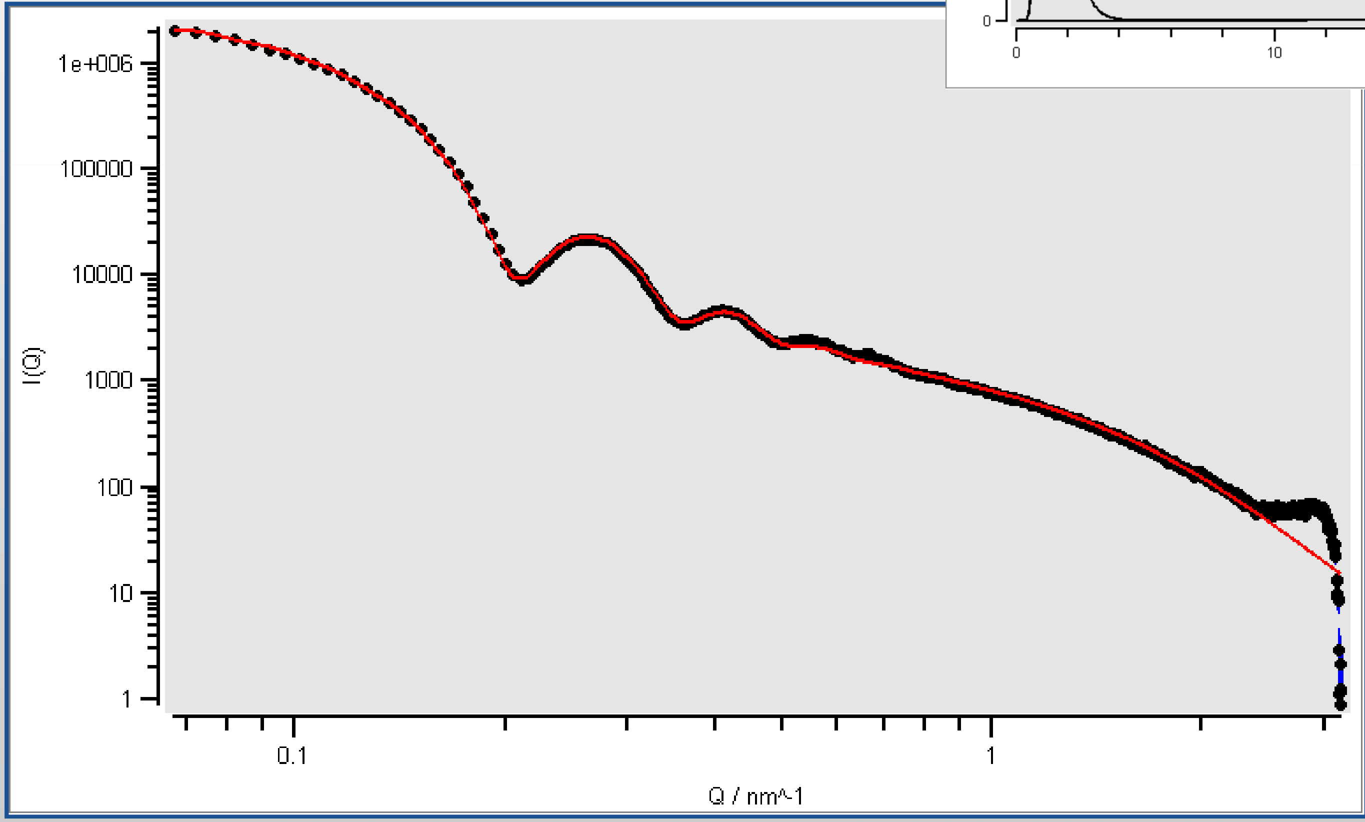

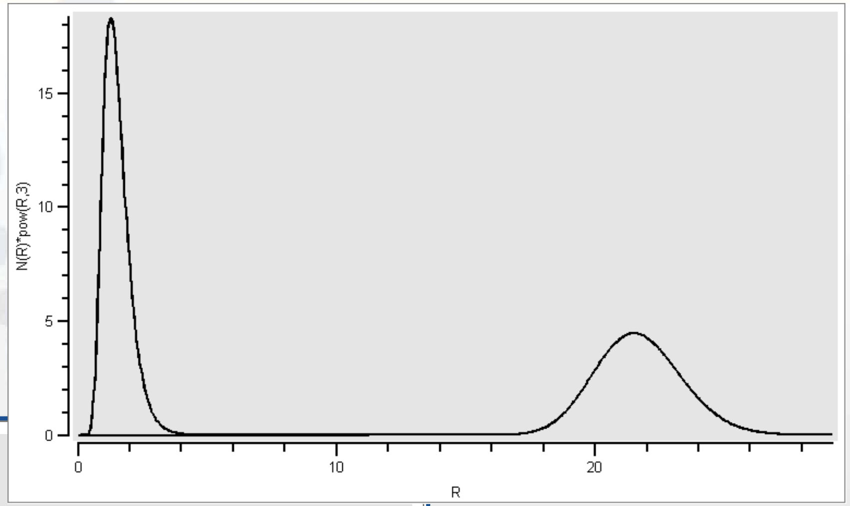

H.B. Stanley *et al.*

Focussing

- Best resolution with a 1d or 2d PSD is obtained by focussing the beam onto the detector
- Traditionally via a curved metal-coated mirror (set at grazing incidence)
- With an undulator, refractive lenses can be employed because the high horizontal collimation directs much of the beam into the lens's limited aperture.

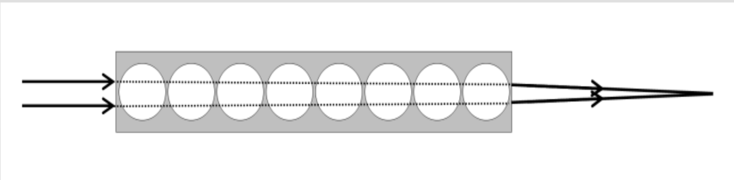

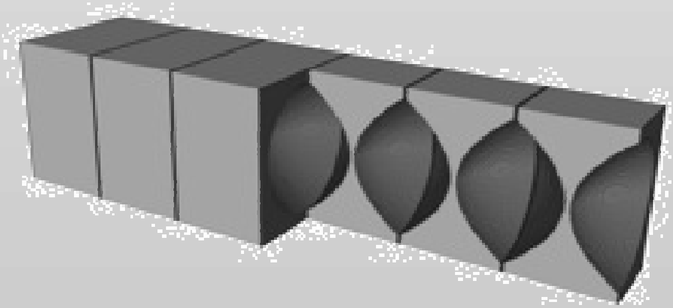

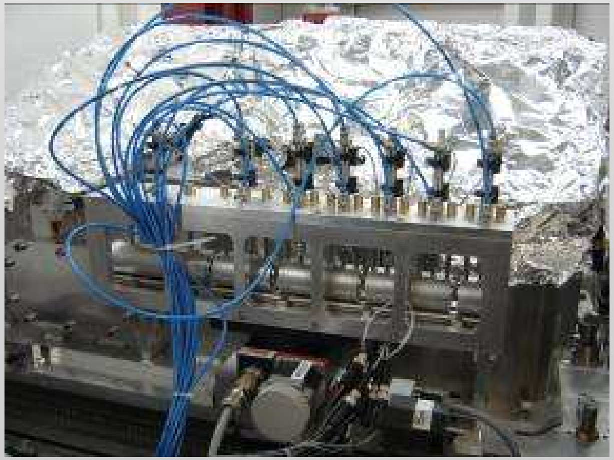

Life at the beamline

- Synchrotron experiments are (often) hard work
- Many samples, quick scans, varying sample conditions, long days and longer nights
- Need to minimise human intervention; maximise automation
- To collect accurate data fit for purpose requires keeping on top of things

- 1) Use the 11-BM mail-in service and let an expert-designed system run it
- 2) Robotic sample changers
- 3) Auto aligning capillaries

ID31's robotic sample changer

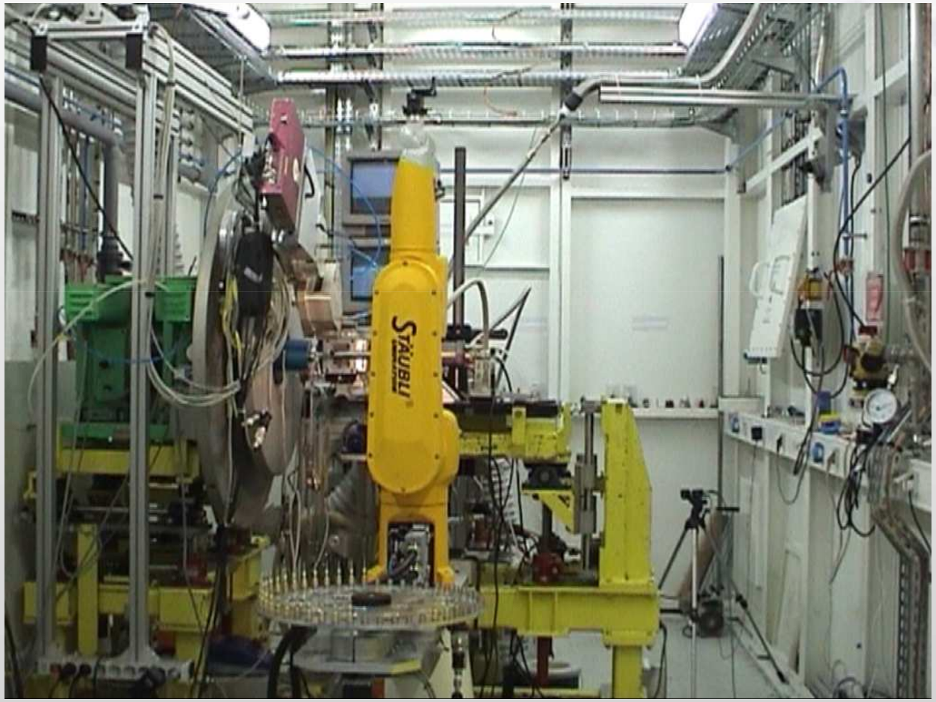

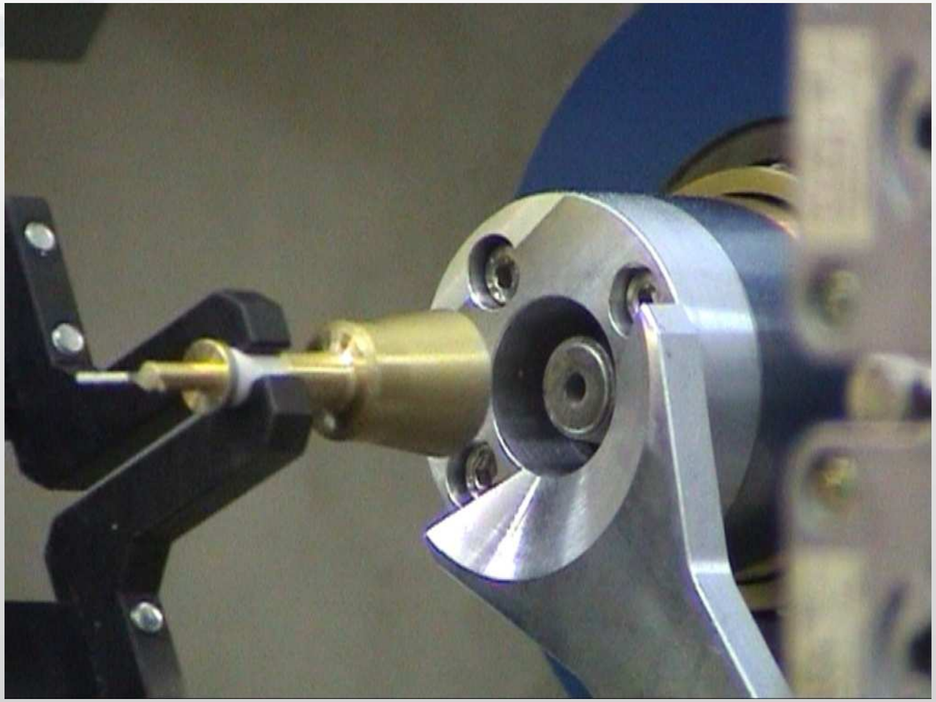

Robots also at 11-BM; Swiss Light Source; I11

45 capillaries filled and ready to run

I11

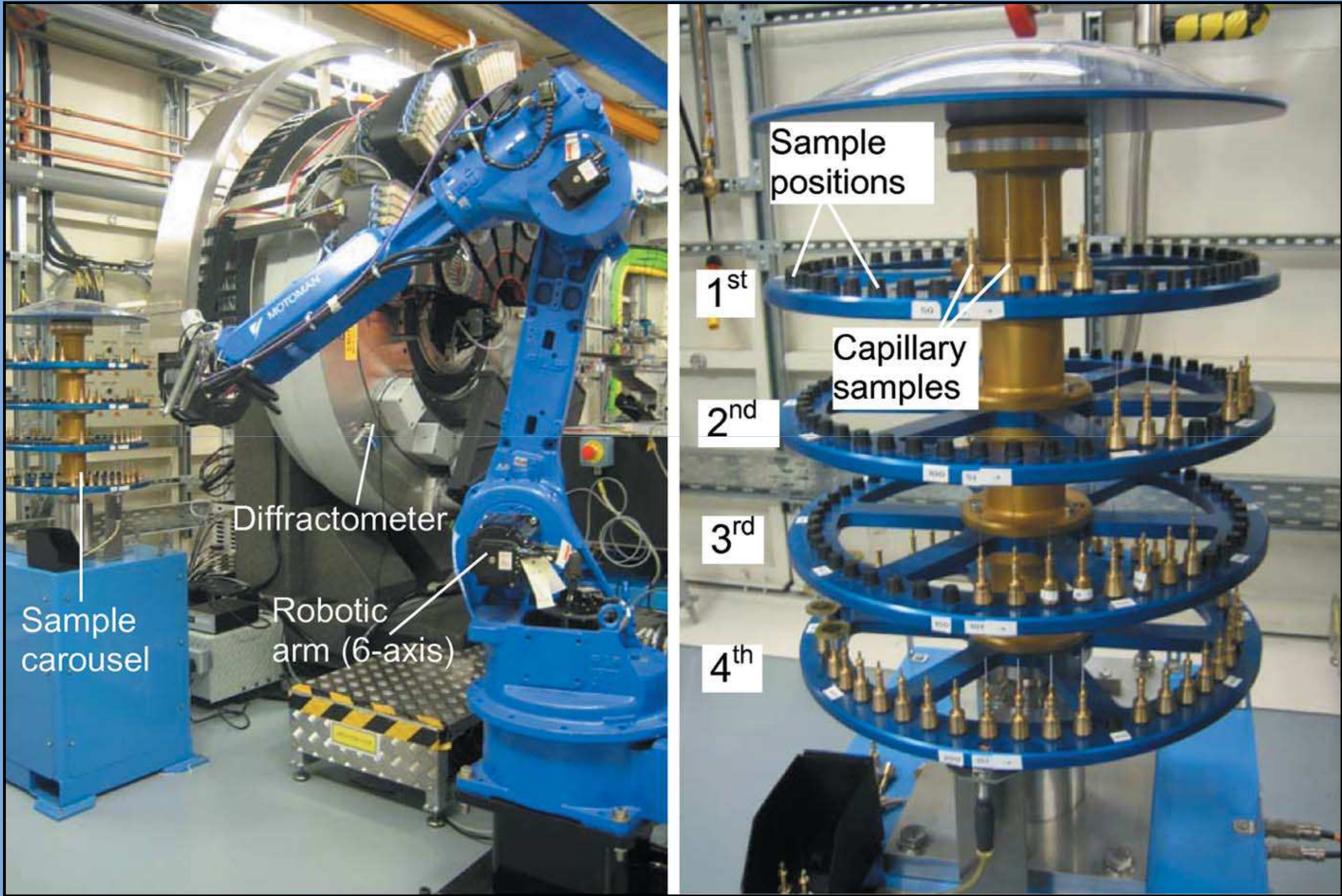

Parker *et al.* J. Appl. Cryst. (2011) 44, 102

Auto capillary spinner alignment

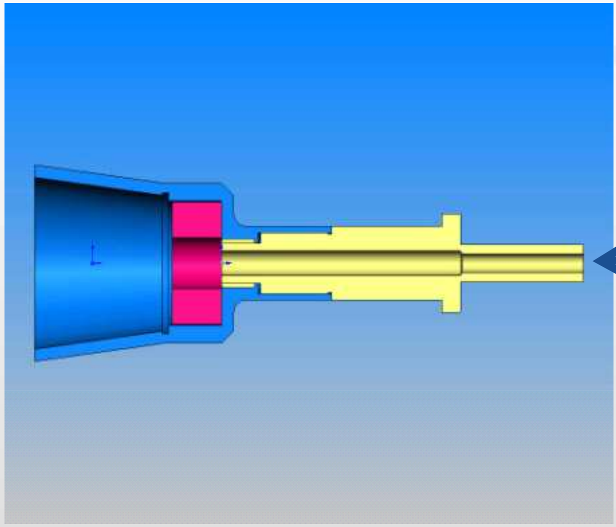

Precision hole to fit capillary

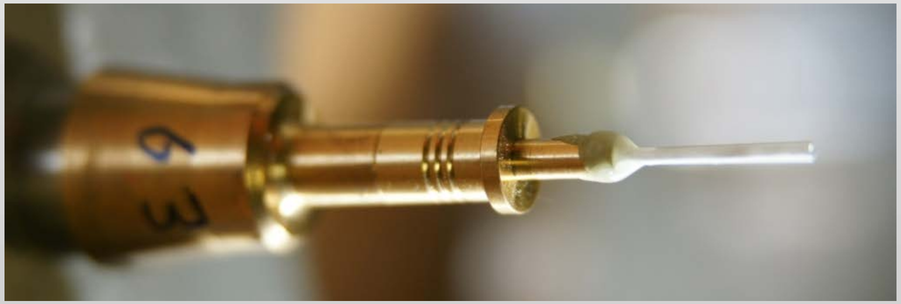

Good enough for analyser crystal

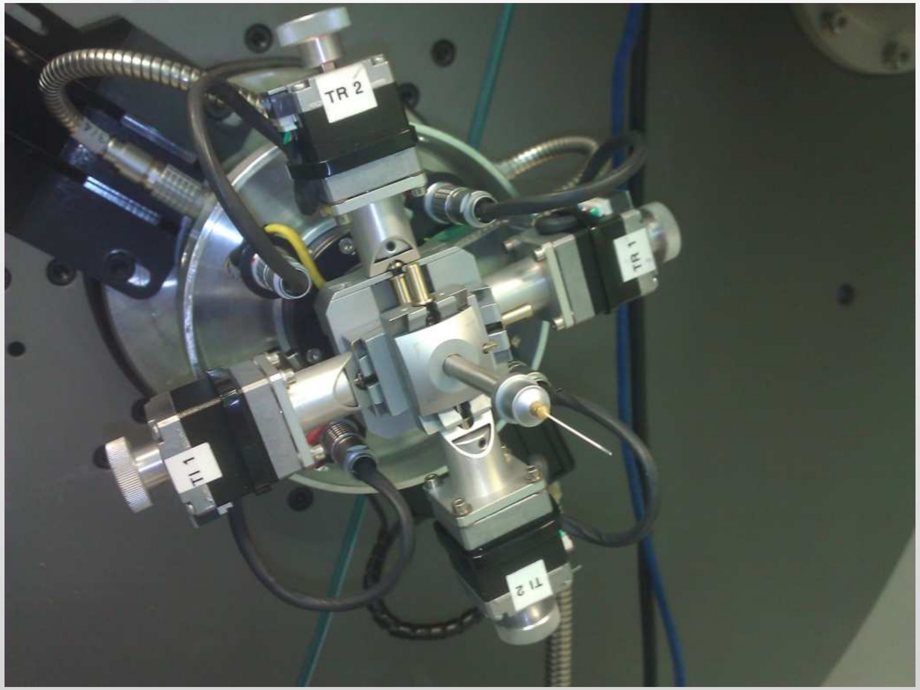

Video-controlled goniometer head at Australian synchrotron; excellent alignment essential for Mythen or other PSD.

I11: Automatic capillary filler; “48 capillaries in 30 mins”

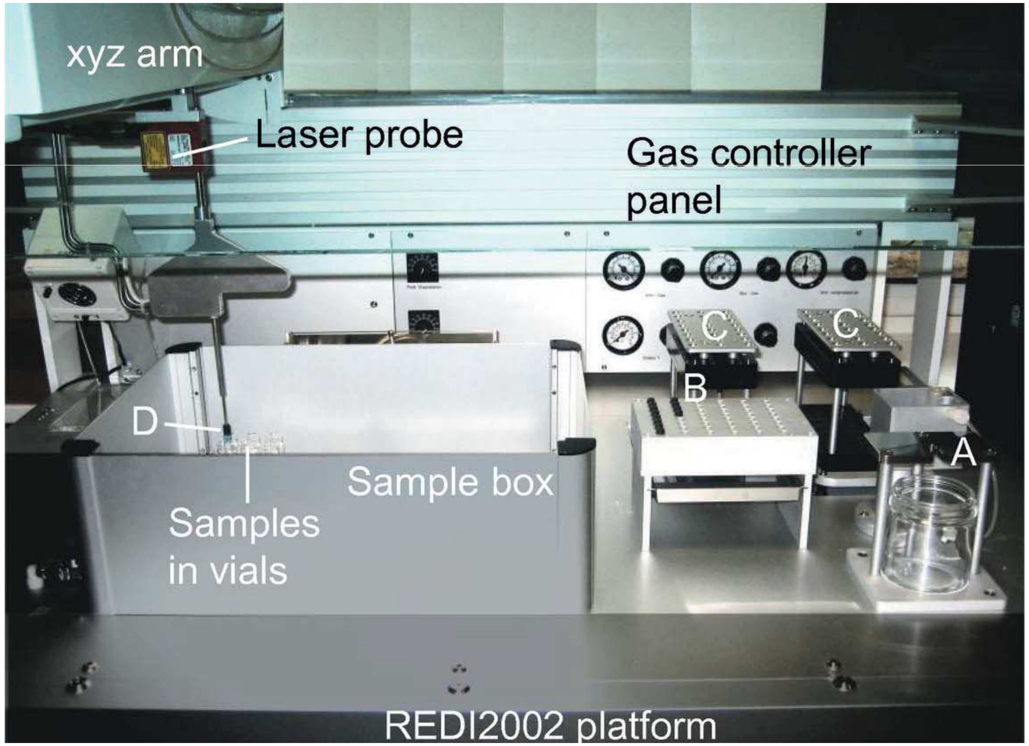

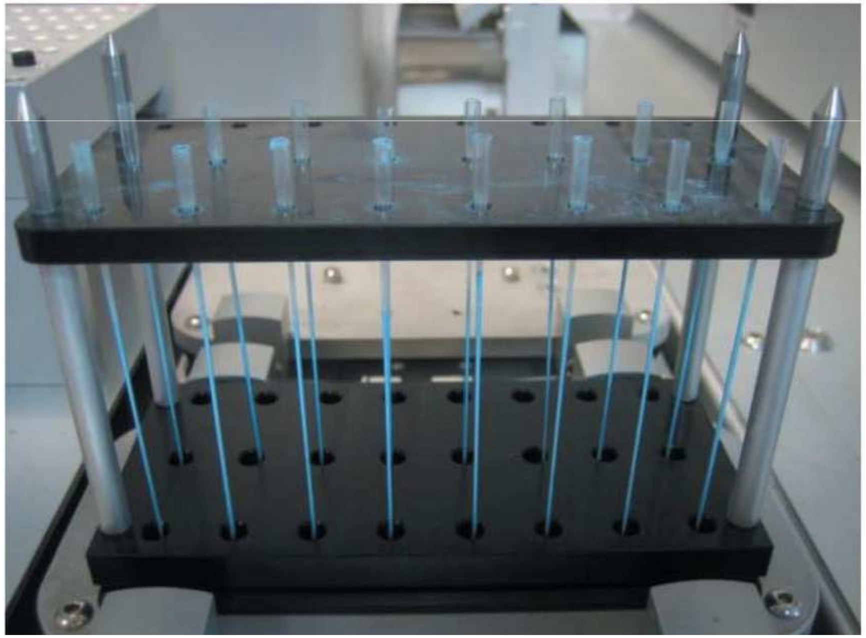

Parker *et al.* J. Appl. Cryst. (2011) 44, 102

Radiation damage

- High photon densities (ID31 has ≈1.5×10^{12} mm^{-2} s^{-1}) at 31 keV
- Even greater flux at softer energies where absorption is also higher
- Loss of peak intensity, peak broadening, and anisotropic shifts in positions
- Really complicates things

Radiation Damage

(certain organics, proteins, organometallics)

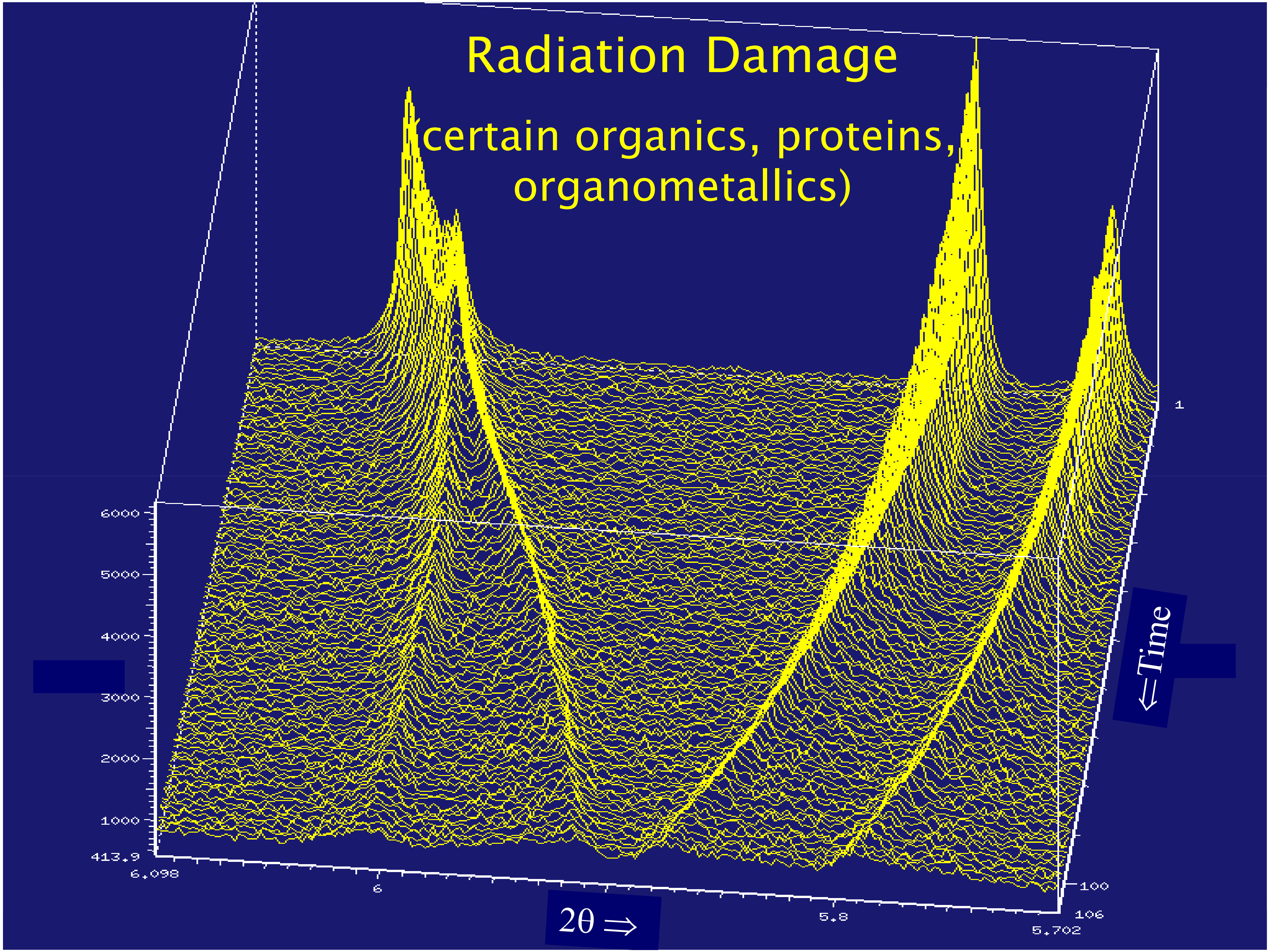

Automatic sample translation between scans to expose fresh sample to the beam.

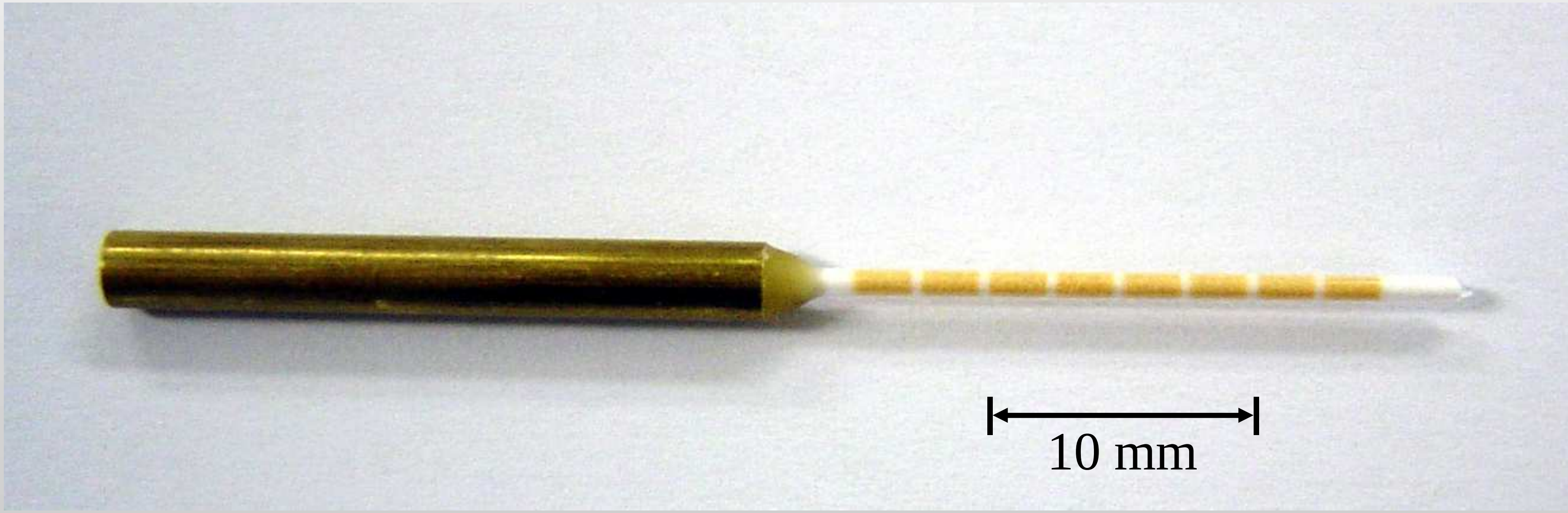

Anisotropic peak shifts can use useful

- because they change the degree of overlap between reflections increasing the overall information content, (c.f. anisotropic thermal expansion, Shankland *et al*. 1997)

- Exploited by Margiolaki *et al*., e.g. in solving and refining SH3 domain of protein “Ponsin”

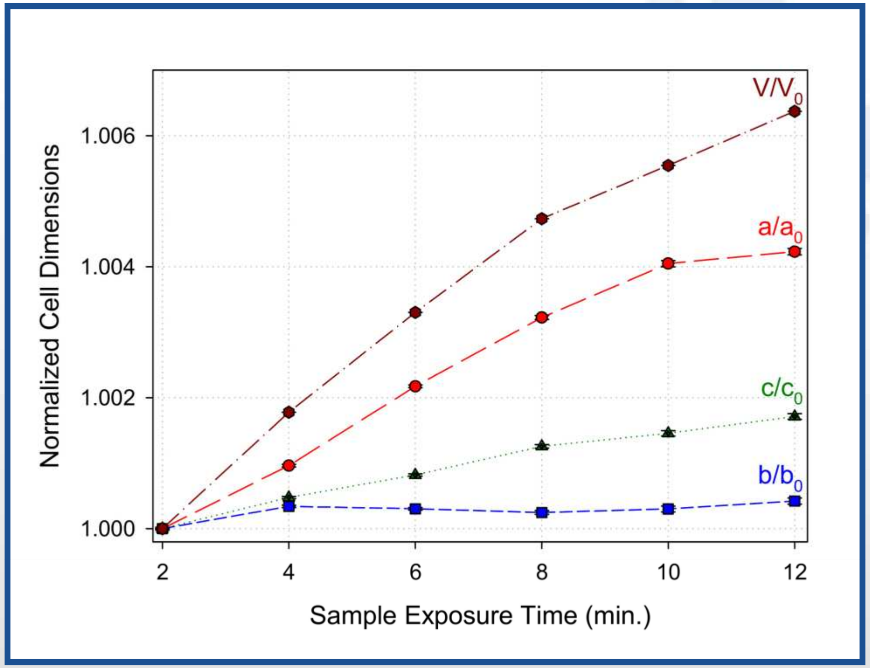

Ponsin: variation of lattice parameters with exposure

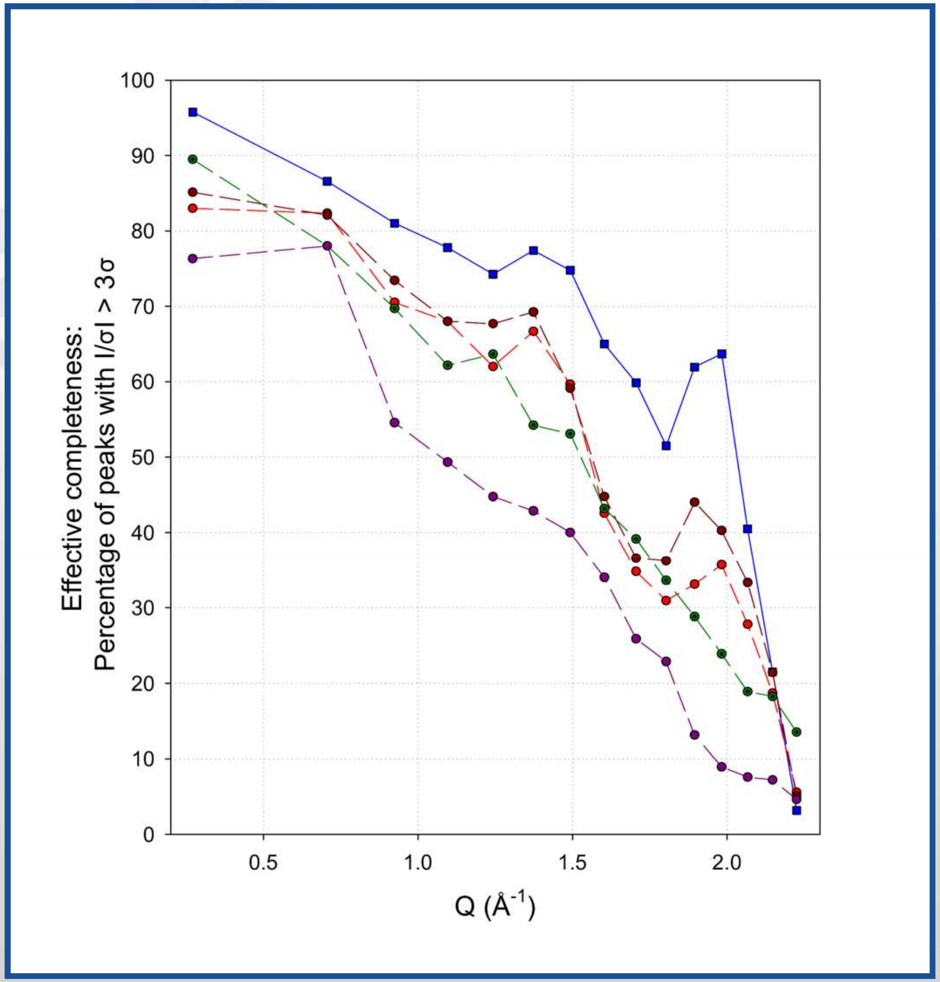

Degree of "completeness" with increasing number of datasets

$P2_12_12_1$
a = 24.7066(4) Å
b = 36.4304(6) Å
c = 72.1058(10) Å

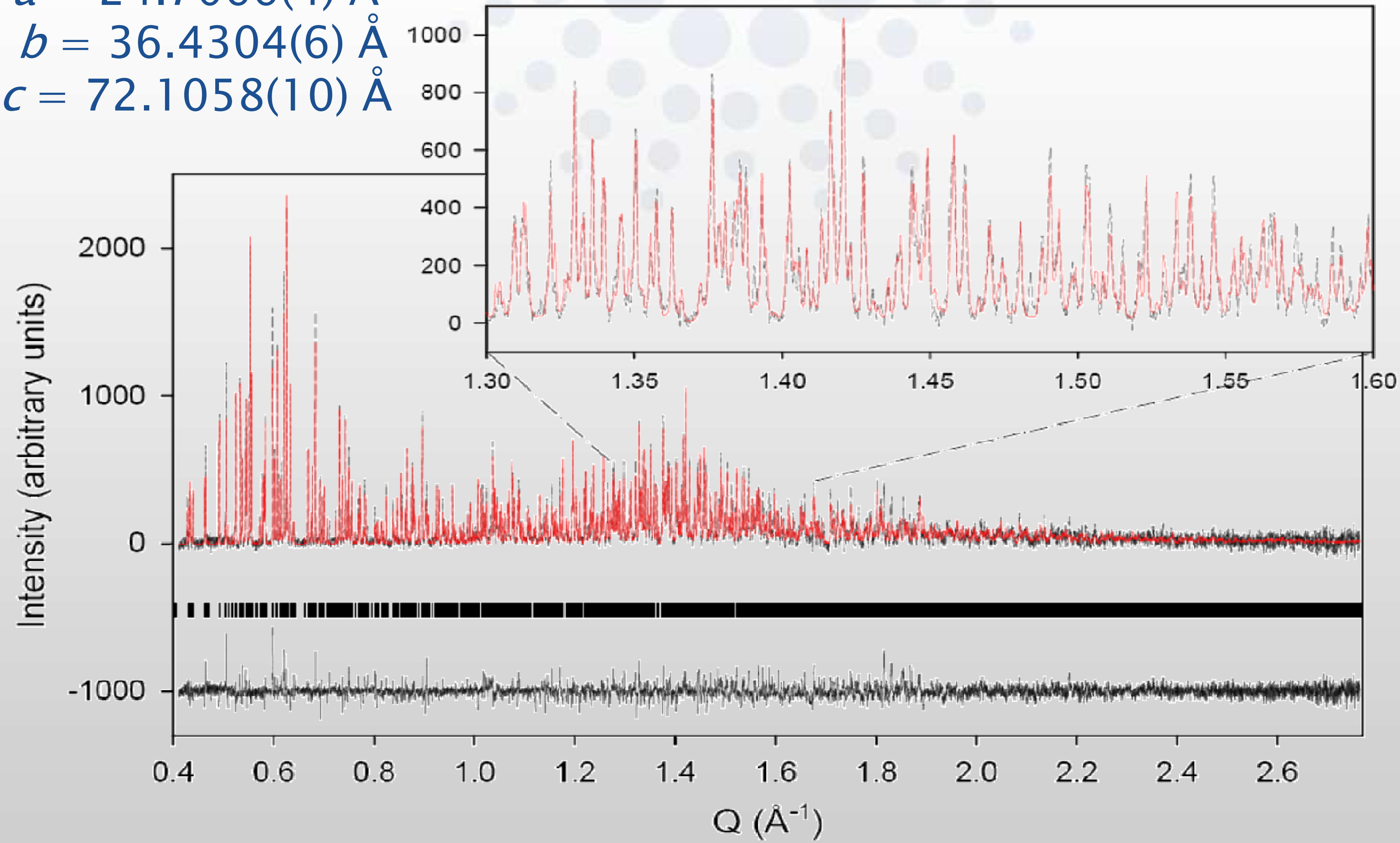

Beam heating

- This can be a problem at low temperature

- Consider a 31 keV beam with 10^{12} photons $mm^{-2}\ s^{-1}$
- μ for Si = 0.31 mm^{-1} (so normally we'd ignore it)
- A 1μm^3 cube intercepts 10^6 photons and absorbs 310 s^{-1}
- Absorbed power = 1.54×10^{-12} W
- Mass of Si cube = 2.33×10^{-15} kg
- Specific heat capacities: 300 K = 704.6 J $kg^{-1}\ K^{-1}$
  10 K = 0.3 J $kg^{-1}\ K^{-1}$
- Heating rate: 300 K = 0.9 K s^{-1}
  10 K = 2200 K s^{-1}

- Obviously absurd prediction!
- Some energy is lost by re-emission (20%)
- and by the gas surrounding the grains transporting heat to the capillary walls.

PROBLEM

- Seal your capillary under air, N_2, Ar, etc, these solidify below ≈50 K leaving a vacuum in the capillary.
- On ID31 we have seen diffraction patterns from sealed capillaries behave wholly unpredictably at low temperatures;
  weird peak shifts; broadening, irreproducible behaviour.

SOLUTION

- Seal capillaries under He, or leave unsealed to allow entry of He exchange gas in the cryostat

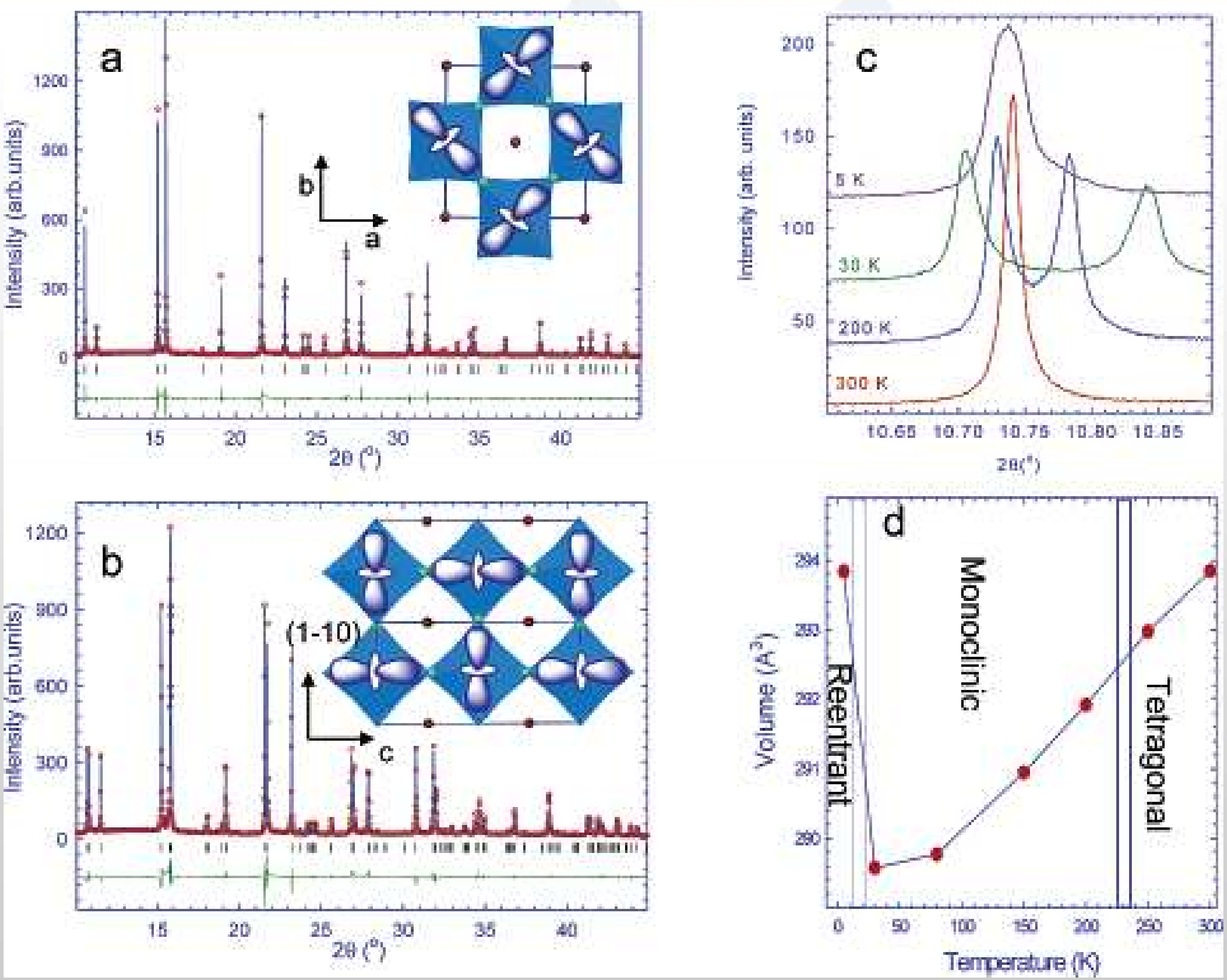
a
b
a
Intensity (arb.units)
2θ (°)
b
(1-10)
c
c
Intensity (arb. units)
5 K
30 K
200 K
300 K
2θ(°)
d
Monoclinic
Reentrant
Tetragonal
Volume (Å3)
Temperature (K)

ID31 is moving in late 2013 to ID22

- Reduced horizontal divergence ⇒ more photons on the sample
- In-vacuum undulator ⇒ more flux at 30 – 40 keV; increase upper energy range from 63 keV (now) to 80 keV (90 keV ??)
    - improved data for absorbing samples, PDF analysis, studies at lanthanide K edges (e.g. for lanthanide glasses), strain mapping, etc.
    - penetration into steels (as well as Ti and Al), dense ceramics, etc.

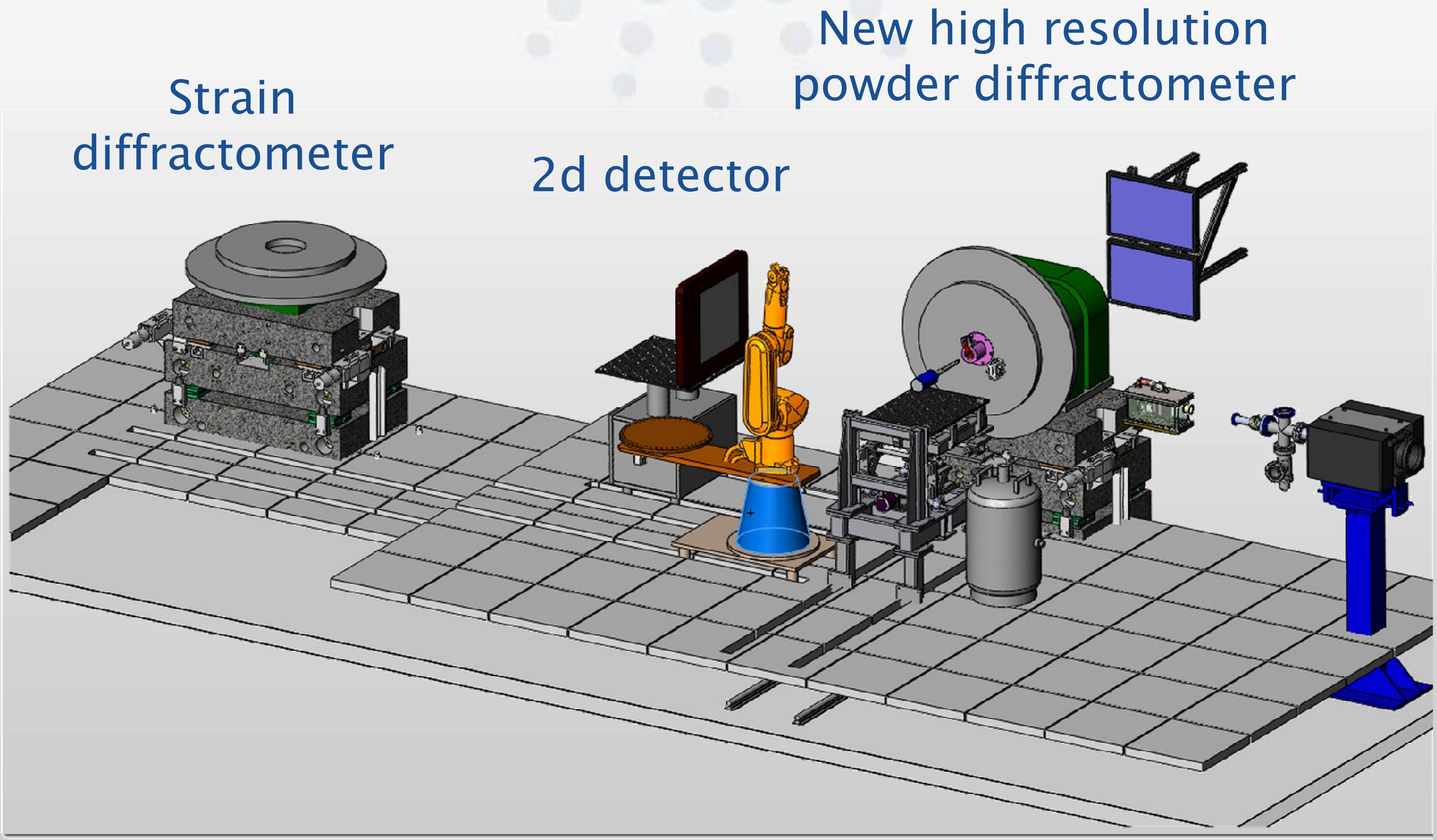
Strain
diffractometer
2d detector
New high resolution
powder diffractometer

Summary

- Explosion of new facilities and beamlines, offering
- high resolution and accuracy via multianalyser stages;
- very fast acquisition / excellent statistics via Mythen or 2d detectors;
- Some of the latest machines offer both capabilities.
- Experiments are done with intermediate or hard energies ($\lambda \leq 1$ Å, $\lambda \leq 0.41$ Å) exploiting insertion device sources where possible.
- Watch out for radiation damage, and beam heating at low T.
- Don't forget it's only powder X-ray diffraction data (so don't over-interpret in the analysis).